The Meteoritical Society

Meteoritics & Planetary Science 1–28 (2016)
doi: 10.1111/maps.12668

Fluids during diagenesis and sulfate vein formation in sediments at Gale crater, Mars

S. P. SCHWENZER[1,2,*], J. C. BRIDGES[3], R. C. WIENS[4], P. G. CONRAD[5], S. P. KELLEY[1], R. LEVEILLE[6], N. MANGOLD[7], J. MARTÍN-TORRES[8,9], A. MCADAM[5], H. NEWSOM[10], M. P. ZORZANO[8,11], W. RAPIN[12], J. SPRAY[13,14], A. H. TREIMAN[2], F. WESTALL[15], A. G. FAIRÉN[16,17], and P.-Y. MESLIN[18]

[1]Department of Environment, Earth and Ecosystems, The Open University, Milton Keynes MK7 6AA, UK
[2]Lunar and Planetary Institute, 3600 Bay Area Blvd., Houston, Texas 77058, USA
[3]Space Research Centre, Department of Physics and Astronomy, University of Leicester LE1 7RH, UK
[4]Space Remote Sensing, Los Alamos National Laboratory, Los Alamos, New Mexico 87544, USA
[5]NASA Goddard Space Flight Center, Greenbelt, Maryland, USA
[6]Canadian Space Agency, St-Hubert, Québec J3Y 8Y9, Canada
[7]Laboratoire Planétologie et Géodynamique de Nantes, LPGN/CNRS UMR6112 and Université de Nantes, 44322 Nantes, France
[8]Luleå University of Technology/Department of Computer Science, Electrical and Space Engineering, Kiruna, Sweden
[9]Instituto Andaluz de Ciencias de la Tierra (CSIC-UGR), Granada, Spain
[10]Institute of Meteoritics and Department of Earth and Planetary Sciences MSC03-2050, 1 University of New Mexico, Albuquerque, New Mexico 87131, USA
[11]Centro de Astrobiología (CSIC-INTA), Torrejón de Ardoz, Madrid, Spain
[12]Université de Toulouse, UPS-OMP, Toulouse, France
[13]Institut de Recherche en Astrophysique et Planétologie, CNRS, UMR 5277, Toulouse, France
[14]Planetary and Space Science Centre, University of New Brunswick, 2 Bailey Drive, Fredericton, New Brunswick E3B 5A3, Canada
[15]Centre de Biophysique Moléculaire, CNRS, Rue Charles Sadron, 45071 Orléans Cedex 2, France
[16]Department of Planetology and Habitability, Centro de Astrobiología (CSIC-INTA), Madrid 28850, Spain
[17]Department of Astronomy, Cornell University, Ithaca, New York 14853, USA
[18]Université de Toulouse, UPS-OMP, IRAP, 31028 Toulouse, France
[*]Corresponding author. E-mail: susanne.schwenzer@open.ac.uk

(Received 06 December 2015; revision accepted 21 March 2016)

Abstract–We model the fluids involved in the alteration processes recorded in the Sheepbed Member mudstones of Yellowknife Bay (YKB), Gale crater, Mars, as revealed by the Mars Science Laboratory Curiosity rover investigations. We compare the Gale crater waters with fluids modeled for shergottites, nakhlites, and the ancient meteorite ALH 84001, as well as rocks analyzed by the Mars Exploration rovers, and with terrestrial ground and surface waters. The aqueous solution present during sediment alteration associated with phyllosilicate formation at Gale was high in Na, K, and Si; had low Mg, Fe, and Al concentrations—relative to terrestrial groundwaters such as the Deccan Traps and other modeled Mars fluids; and had near neutral to alkaline pH. Ca and S species were present in the 10^{-3} to 10^{-2} concentration range. A fluid local to Gale crater strata produced the alteration products observed by Curiosity and subsequent evaporation of this groundwater-type fluid formed impure sulfate- and silica-rich deposits—veins or horizons. In a second, separate stage of alteration, partial dissolution of this sulfate-rich layer in Yellowknife Bay, or beyond, led to the pure sulfate veins observed in YKB. This scenario is analogous to similar processes identified at a terrestrial site in Triassic sediments with gypsum veins of the Mercia Mudstone Group in Watchet Bay, UK.

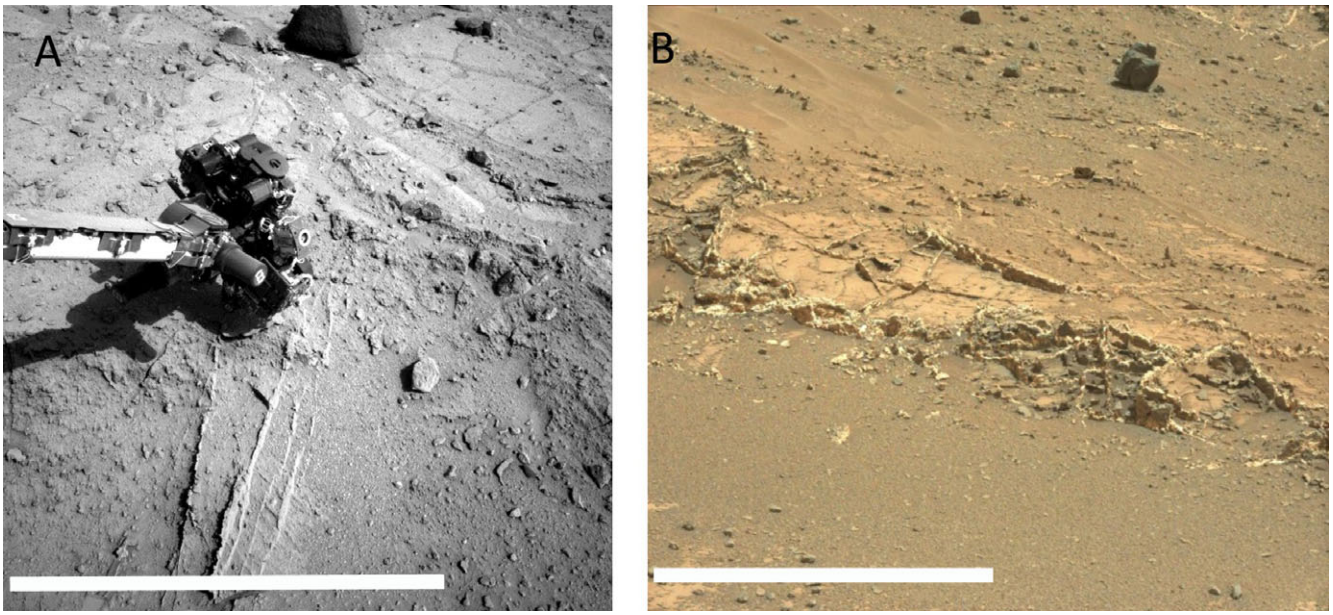

Fig. 1. A) Sulfate veins prominent at Darwin outcrop veins, observed on sol 402, NavCam NRB_432923862. Field of view 1.3 m. B) Garden City image, observed on sol 924, MastCam ML004061. White sulfate veins cut through the surrounding sediments. Scale bars are 1 m.

INTRODUCTION

Fluids are very important factors in geologic processes, prompting H. P. Eugster to coin the phrase "behind every important mineral there once was a fluid" (Eugster 1986), and fluids are equally important for life, because they are the source and transport medium for nutrients. Water is one of the essential ingredients for life, but more information is needed to understand if Mars in the past was habitable for microbial life (Conrad 2014). Physical characteristics, e.g., the irradiation environment and temperature, need to be considered (Conrad 2014). For fluids, the most important criteria, apart from providing liquid water, are the temperature, pH, redox potential (energy source), and composition, as well as the duration of water-related processes in the Martian crust [Brack et al. 2010; Fairén et al. 2010a, 2010b; Cockell et al. 2012; Westall et al. 2015). Therefore, the exploration of Mars has focused many investigations on finding signs of past and present water. Those investigations have returned firm evidence for the past presence for water from landed missions (e.g., Squyres et al. 2004, 2008, 2012; Grotzinger et al. 2005; Tosca et al. 2008; Smith et al. 2009), orbiter near IR spectral measurements (Bibring et al. 2005; Mustard et al. 2008), photographic imagery (e.g., Carr [2006] for review), and the SNC meteorites (Harvey and McSween 1996; Bridges et al. 2001; Treiman 2005; Changela and Bridges 2010; Hallis and Taylor 2011; Hicks et al. 2014). The Curiosity Rover of the Mars Science Laboratory (MSL) mission is no exception in trying to find and understand signatures of water-related processes at Gale crater on Mars.

After imaging conglomerates within the first weeks after landing in Gale crater (Williams et al. 2013a, 2013b), MSL detected light-toned veins about 450 m away from Bradbury landing (Fig. 1) in the Sheepbed member of the Yellowknife Bay formation, including the John Klein Drill hole (Fig. 2). Southeast of the conglomerates, the rover entered into the stratified sediments of the Yellowknife Bay formation, which is divided into (top to base) an ~3 m thick unit consisting of the Gillespie and Glenelg members and the ≥1.5 m thick Sheepbed member (Grotzinger et al. 2014). The veins were first identified in the Glenelg and Gillespie members (encountered on sols 113–125), which are coarse sandstones with local pebbles, but are more developed inside the underlying Sheepbed member studied from sols 126 to 300 (Nachon et al. 2014). The Sheepbed member is a mudstone with 22% clay and 28% amorphous phases (John Klein drill fines; Vaniman et al. 2014). The light-toned veins are not the only signs of syn- and post-depositional alteration and diagenesis in the Sheepbed member: early diagenetic features are Mg-rich veins, referred to as raised ridges (Leveille et al. 2014; Siebach et al. 2014), and solid, hollow, and sulfate-filled nodules (Stack et al. 2015).

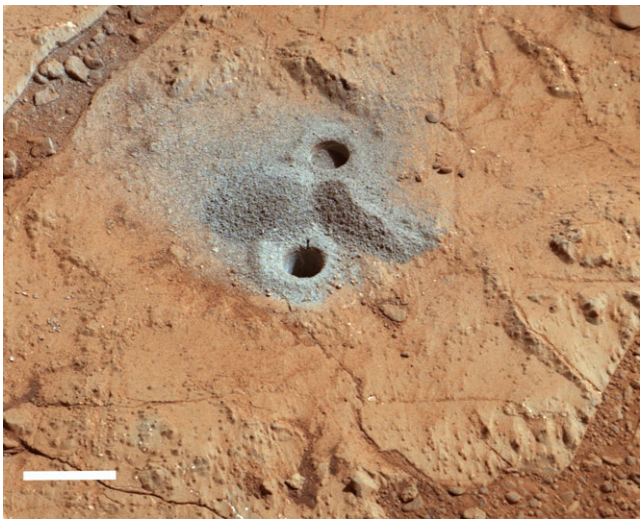

Fig. 2. Drill hole into the John Klein target within Sheepbed Member of Yellowknife Bay, with a light-toned sulfate veinlet visible on the back wall. The light-toned veins have been identified as sulfates by ChemCam (Nachon et al. 2014; Schroeder et al. 2015) and CheMin (Vaniman et al. 2014). Drill hole is 1.6 cm diameter. Image is white balanced. Scale bar is 2 cm (NASA image PIA16815_Fig 1_WB_unannotated-full).

The raised ridges are interpreted to have formed before lithification of the Sheepbed mudstone, and the solid and hollow nodules are interpreted as either contemporaneous with the raised ridges or slightly later —depending on the preferred model for their formation. However, all models favor early diagenetic formation (Leveille et al. 2014; Siebach et al. 2014; Stack et al. 2015). The light-toned veins crosscut the raised ridges and are thus younger. Similarly, the light-toned infill in the filled nodules is younger than the formation of the hollow nodules (Stack et al. 2015). These observations taken together record a history of deposition within a fluvio-lacustrine environment followed by low-temperature alteration (Grotzinger et al. 2014).

Since the Yellowknife Bay observations, Curiosity has driven over 10 km toward the lower parts of Mt. Sharp. Along the route, more sulfate veins have been identified at different outcrops throughout the stratigraphy and in different lithologies, including coarse sandstones and conglomerates (Vasavada et al. 2014). The veins are most abundant in fine-grained facies and are particularly prominent in the Pahrump facies composed predominantly of fine-grained sandstones (Kronyak et al. 2015; Stack et al. 2015).

The light-toned veins have been identified as nearly pure Ca-sulfate by ChemCam laser induced breakdown spectroscopy (LIBS) and alpha particle X-ray spectrometry (APXS) analyses (McLennan et al. 2014; Nachon et al. 2014). ChemCam detected hydrated Ca-sulfates in 55 individual analysis points corresponding to a total of 24 distinct veins distributed in all members of the Yellowknife Bay formation (table 1 in Nachon et al. 2014), e.g., at targets named "Reddick Bight" and "Denault" on sols 316 and 317 (Anderson et al. 2014). The hydration state of the light-toned fracture fills is consistent with hydrated Ca-sulfates. Rapin et al. (2015) used H analyses by LIBS to show that the veins were predominantly bassanite ($2CaSO_4 \times H_2O$), i.e., sulfate in a less hydrated state than gypsum ($CaSO_4 \times 2H_2O$). Notably, the only trace element observed in the sulfate veins by ChemCam is Sr, which readily substitutes for Ca, but other elements typically associated with Ca-sulfates, e.g., Ba, Rb, Zn, and others, have not been not detected (Nachon et al. 2014), indicating a pure Ca-sulfate as might result from recrystallization of a previous deposit.

Drilling of the mudstone (John_Klein and Cumberland) revealed a light-toned vein in the John Klein drill hole (Fig. 2) and allowed analysis of material in the CheMin instrument by X-ray diffraction (Vaniman et al. 2014) and also by pyrolysis with the SAM instrument (Ming et al. 2014). Sulfates were detected by CheMin, which found anhydrite and bassanite (Vaniman et al. 2014) in the John Klein drill fines that are consistent with the presence of light-toned veins observed on the drill walls, but could also be a mixture of matrix and vein material. The SAM measurements of the drill fines released SO_2 and H_2S, but Ca-sulfates usually decompose at higher temperatures than are achievable with the SAM oven, and therefore, other sulfur-bearing phases (e.g., sulfides) in the sample are responsible for these gas evolutions (Ming et al. 2014). Sulfates have further been found in filled nodules (Stack et al. 2015), with the filling being interpreted as late in the diagenetic sequence. The current scenario is that first a hollow formed and was subsequently partially or entirely filled to form a nodule because, in most cases, a hairline fissure connecting the filled nodule with a sulfate vein can be observed (Grotzinger et al. 2014; Stack et al. 2015).

Crosscutting relationships show that sulfate formation postdates the formation of clays. We have modeled the clay formation though incongruent dissolution of Martian bedrock at Yellowknife Bay (Bridges et al. 2015). Here, we use those results to address the composition of the fluid that resulted from this clay formation and compare the Gale crater fluid to fluids derived from alteration of a range of Martian compositions. In this new study, we also test the hypothesis that the clay-forming fluid subsequently precipitated the sulfates and discuss the precipitation

Table 1. Fluids forming clay minerals in Gale crater rocks. Fluids are extracted from models that evaluate the formation of clays in Yellowknife Bay (Bridges et al. 2015). Mix is a mixture of 70% olivine, 20% Portage amorphous, and 10% Portage whole rock. Portage soil, Ekwir, and Jake_M rocks were measured in the Yellowknife Bay area. wr denotes whole rock; am, an amorphous component. Data from Gellert et al. (2013); Morris et al. (2013, 2014); Stolper et al. (2013); Schmidt et al. (2014); for details see also Bridges et al. (2015).

	Mix	Mix	Portage am	Portage am	Portage wr	Portage wr	Ekwir wr	Ekwir wr	Jake_M wr	Jake_M wr
Species	W/R 1000	W/R 100	W/R 1000	W/R 100	W/R 1000	W/R 100	W/R 1000	W/R 100	W/R 1000	W/R 100
Cl^-	2.16E-03	5.62E-03	2.08E-03	4.80E-03	1.98E-03	3.81E-03	2.30E-03	6.91E-03	2.03E-03	4.31E-03
HCO_3^-	1.68E-05	1.68E-05	1.68E-05	1.68E-05	1.68E-05	1.68E-05	1.68E-11	1.68E-11	1.68E-05	1.68E-05
S*	3.85E-03	2.87E-03	3.98E-03	4.24E-03	3.79E-03	2.10E-03	3.72E-03	1.36E-03	3.97E-03	4.29E-03
HPO_4^{2-}	4.07E-13	9.32E-13	5.53E-13	5.07E-12	6.06E-13	1.86E-11	5.63E-13	1.07E-11	1.00E-09	4.72E-05
K^+	7.19E-04	8.35E-04	4.34E-04	1.93E-04	1.79E-04	3.05E-05	1.86E-04	3.78E-05	3.44E-04	1.27E-05
Na^+	9.67E-03	1.29E-02	1.05E-02	1.88E-02	1.01E-02	1.69E-02	1.01E-02	1.66E-02	1.15E-02	3.26E-02
Mg^{2+}	2.65E-09	1.02E-09	2.41E-09	3.67E-10	2.83E-09	1.73E-10	3.01E-09	2.64E-10	5.32E-11	7.31E-13
Ca^{2+}	5.30E-04	2.25E-04	4.75E-04	6.85E-05	5.10E-04	2.32E-05	5.42E-04	3.58E-05	3.26E-06	2.27E-09
Al^{3+}	1.82E-11	2.45E-11	3.43E-11	7.63E-11	4.56E-11	1.63E-10	4.42E-11	1.25E-10	6.07E-07	2.62E-05
Fe**	7.78E-09	1.44E-08	3.38E-09	1.28E-08	1.50E-09	7.91E-09	1.44E-09	6.30E-09	4.01E-10	2.52E-09
SiO_2(aq)	7.58E-04	1.46E-03	1.04E-03	3.65E-03	1.14E-03	6.28E-03	1.11E-03	5.02E-03	4.05E-04	6.02E-03

*sum of all S species, **sum of all Fe in Fe species.

mechanisms of pure sulfate from the Yellowknife Bay fluid and comparable brines.

METHODS

We build on the results obtained in our earlier work on the Yellowknife Bay rocks at Gale (Bridges et al. 2015), the nakhlite Martian meteorites (Bridges and Schwenzer 2012), and impact-generated hydrothermal systems (Schwenzer and Kring 2009, 2013; Bridges and Schwenzer 2012; Schwenzer et al. 2012a, 2012b; Filiberto and Schwenzer 2013). For the thermochemical modeling in all cases, we applied the code CHIM-XPT (previously CHILLER; Reed and Spycher 2006; Reed et al. 2010), which has been used extensively in terrestrial basaltic environments (e.g., Reed 1982, 1983) and has been applied to Martian compositions (DeBraal et al. 1993). For Gale crater, we tested two different types of starting fluids with varying redox characteristics (Bridges et al. 2015): "adapted water" (AW) and "Gale portage water oxidized" (GPWox), to arrive at alteration mineral assemblages produced from fluid–rock interaction at low temperatures. The difference in the two fluids is that AW is a "generic" Martian fluid generated from terrestrial fluid compositions (Deccan Traps; Minissale et al. 2000) and adapted to Mars (for details, see the Model Conditions section and Schwenzer and Kring 2009), while GPWox is a fluid created from the model reaction of Portage Soil, as measured at Gale, with a very dilute fluid. For details, see the 'Model Conditions' section and our previous study (Bridges et al. 2015). The focus of the previous study was on the alteration minerals, while here we focus on the fluids. We will compare the Yellowknife Bay fluids to other Martian fluid compositions from our own studies and from the literature (see the 'Fluids from the Literature: Analogs, Experiments, and Models' section and results).

Model Conditions

A detailed discussion of the model conditions and input parameters is given in Bridges et al. (2015). Results of calculated equilibrium mineral assemblages are presented in diagrams of mineral abundance versus W/R ratio (mass of rock reacted with the starting fluid). W/R is a progress variable with very limited rock dissolution at the high W/R end and increased rock dissolution at the low W/R end. The amount of alteration minerals precipitated increases from a few mg at very high W/R to about 1 g at W/R of 1000 and on the order of 10 g of rock at W/R of 100. Note that the model W/R represents the amount of rock reacted with a fluid on Mars, not the total amount of rock present in a given volume of rock on Mars. Two important parameters are redox and the sulfur content during alteration. In the representative cases considered here, the solution is initially oxidizing (all S species as SO_4^{2-}). The SO_4^{2-}/HS^- pair controls redox in the fluid, and a set of 112 different ionic species are typically used to represent the fluid chemistry in each calculation step. The sulfur concentration of Deccan Trap fluids (Minissale et al. 2000) was adopted for our model, and chlorine was used as the charge balance ion.

Both S and Cl are also contained in the rocks, and therefore, their concentrations increase as the model calculation progresses from high to low W/R. This, in turn, can lead to higher activities in solution (Cl) or higher amounts of precipitate (S). The Gale materials used for the models in Bridges et al. (2015) were Jake_Matijevic as an alkaline rock endmember; Ekwir_brushed as the average, relatively dust-free, basaltic composition rock endmember; and Portage as the basaltic soil endmember. The latter gave a representative regional composition, but also allowed access to its mineralogy through the CheMin measurements, and therefore enabled the modeling of incongruent dissolution. The Gale rock compositions as measured by APXS were used (Gellert et al. 2013; Stolper et al. 2013; Schmidt et al. 2014) and 10% of the total Fe (molar) was taken as Fe^{3+}, as deduced from redox conditions in Martian meteorites and used in our previous models (see, e.g., Schwenzer and Kring 2009; Filiberto and Schwenzer 2013), but also after testing a wider range of conditions for the specific Gale crater case (Bridges et al. 2015). Three different temperatures, 10 °C, 50 °C, and 150 °C, were modeled because they represent a temperature range relevant to the formation of alteration minerals at Gale crater. The model assumes diagenetic, subsurface conditions, and therefore, the fluid is not in contact with the atmosphere. We focused on the basaltic soil Portage and especially mineral mixtures for our modeling results, but also compare alteration mineral assemblages and fluids resulting from alteration of those to the precipitates and fluids of other basaltic (target Ekwir) and alkaline (target Jake_M) rocks. The mineral mixtures allowed us to consider incongruent dissolution and a direct comparison of phases, e.g., less olivine in clay-rich sediments compared to Portage soil (see Bridges et al. [2015] for details). In these mixtures, Mg and Fe are predominantly delivered by the dissolution of olivine, while alkali elements (Na, K) and Ca and S are sourced from the amorphous phase. For this study, we extract fluids from the Portage alteration models at two different W/R: 100 and 1000 (Table 1). Evaporation is modeled in two different ways (1) water removal without mineral fractionation and (2) water removal with mineral fractionation.

Fluids from the Literature: Analogs, Experiments, and Models

To compare the model results obtained here with fluid compositions from other models and from experimental investigations, we have compiled fluids from the literature (Table 2). There is a large body of literature concerned with alteration of basaltic rocks of terrestrial and extraterrestrial provenance. Here, we select those experimental fluids concerning the modeling of fluids and rocks of Martian compositions (Table 3). Terrestrial analog sites without the influence of seawater are rare. We, therefore, use fluids venting from the Deccan Traps (Minissale et al. 2000) as our main point of comparison, but also compare to fluids from Iceland and other basaltic regions (Table 2). Further, we include a range of dilute terrestrial waters (Table 2) because these offer a wide range of rock and aquifer conditions for comparison. For the evaporation studies, we compare to salt lakes and evaporating water bodies on Earth.

RESULTS

Fluid Compositions in Gale crater

Fluid compositions derived from the alteration of three different whole rocks (Portage soil, Ekwir, and Jake_M, see the Model Conditions section and Bridges et al. [2015] for a host rock discussion); the amorphous component found in Portage soil; and a mix of 70% Portage amorphous phase, 20% olivine, and 10% Portage whole sample ("mix" hereafter) are shown in Table 1 and Fig. 3. Total dissolved solids for all modeled fluids range from 1.8×10^{-2} to 4.7×10^{-2} mole L^{-1}; individual element concentrations are listed in Table 3.

Fluid composition depends on a multitude of factors from dissolving host rock composition to precipitating minerals, all of which are dependent on factors such as temperature and chemistry of an incoming fluid. Figure 3 shows the results of three whole-rock compositions: Portage soil, Ekwir, and Jake_M (see also Bridges et al. 2015) modeled with an incoming, prereaction fluid equilibrated with regional rock (represented by Portage soil, for details see the 'Model Conditions' section of this study and Bridges et al. [2015; Model Conditions section, p. 5]) prior to the clay-forming reactions. All resulting, postreaction fluids are low in Mg and Fe, which is a result of clay formation, whereas the alkali elements Na and K are not notably deposited with the precipitating minerals and therefore accumulate in the fluid. Mg is lowest in Jake_M—and in the fluid corresponding to the complete dissolution of a Jake_M rock composition, whereas Al is highest in the rock and fluid. In contrast, P is high in Jake_M-derived fluids although the rock has the lowest P_2O_5 concentration of all compositions used for this study. This is an effect of mineral formation because with the low Mg concentrations available for clay formation, Na-Ca-zeolite forms in Jake_M alteration assemblages (see Bridges et al. 2015, their Fig. 4) taking up Ca, causing low Ca

Table 2. Compilation of literature data from experiments, analogs, and models, including reference, method, and comments of rock/starting composition used.

	Starting material/ composition/analog site	Method description	Temperature, °C	Reference
Experiments	Columbia River basalt	Flow and batch experiments	23, 75	Baker et al. (2000)
	Mars simulant from single minerals	Long-term batch experiment with gas flow	3, 25, 35	Bullock et al. (2004)
	Los Angeles Martian meteorite analog glass	Batch and flow-through experiments, acidic starting fluid	75	Hurowitz et al. (2005)
	Nakhla meteorite	Leaching	24	Sawyer et al. (2000)
	Analog basalt	Leaching and evaporation	25	Tosca and McLennan (2009)
	Analog basalt	Long-term reaction study	20	Moore and Bullock (1999)
	Cerro Negro Volcano basalt	Hydrothermal experiments	65, 150, 200	Marucci and Hynek (2014)
Model	Earth analogs	Theoretical deduction	N/A	Catling (1999)
Analog	Dry Valley, Antarctica	Ancient ground ice	Frozen when sampled	Dickinson and Rosen (2014)
	Deccan Traps	Water venting the basalts	Various	Minissale et al. (2000)
	Ngejepa Wells	Groundwater		Jones et al. (1977)
	Mount Cameroon	Springs and rivers	Surface	Benedetti et al. (2003)
	British bottled waters	Groundwater	Surface	Smedley (2010)
	Mt Etna, Italy	Groundwater	Surface	Aiuppa et al. (2000)
	British Columbia	Lake water	Surface	Hudec and Sonnenfield (1980)
	Kenyan Rift Valley	Borehole water		Jones et al. (1977)
	Iceland	Geothermal waters and hot springs	Various	Arnórsson et al. (1983)
	Various andesitic and basaltic	Geothermal waters and hot springs	Various	Arnórsson et al. (2007)
	Wiesbaden	Thermal spring water	≤70	Loges et al. (2012)
	W North America	Saline lakes	Surface	Drever (1988)
	Botswana	Lakes in arid region	Surface	Eckhardt et al. (2008)
	Various	Lakes in dry areas	Surface	Kempe and Degens (1985)

concentrations in the fluid and preventing apatite formation.

Basaltic compositions, here represented by the Portage soil and the rock target Ekwir, have very similar fluid properties (Table 3). Portage soil fluid at W/R of 1000 during alteration has total dissolved solids (TDS) of 1.77×10^{-2} mole L^{-1}, with the most abundant ions being Na, sulfate, and Cl. At W/R of 100 during alteration, the total dissolved solids are 2.92×10^{-2} mole L^{-1} with the most abundant ions being Na, S species, and Cl.

Ekwir fluid at W/R of 1000 during alteration has a TDS concentration of 1.80×10^{-2} mole L^{-1}, with the most abundant ions being Na, sulfate, and Cl. At W/R of 100 during alteration, the total dissolved solids are 3.00×10^{-2} mole L^{-1} with the most abundant ions being Na, Cl, and SiO_2.

Jake_M rock composition is different from the basaltic compositions because of its high K-content and has been described as a mugearite (Stolper et al. 2014). Thus, the fluid resulting from a reaction of this rock is notably different at lower W/R. At W/R of 1000 during the alteration, this fluid has a TDS concentration of 1.83×10^{-2} mole L^{-1}, with the most abundant ions being Na, sulfate, and Cl. At W/R of 100 during alteration, the total dissolved solids are 4.73×10^{-2} mole L^{-1}, which is the highest TDS value observed (Table 3).

We mainly focus on the "mix" composition because we demonstrated in Bridges et al. (2015) that the dissolution of the host rock was incongruent, and that the alteration of predominantly amorphous component with olivine and whole rock resulted in a clay mineral composition most closely related to the observed clay minerals (Vaniman et al. 2014). The fluid produced during this alteration reaction, therefore, is the most realistic fluid for a Gale pore water fluid. At W/R of 1000 during the alteration, the "mix" fluid has a TDS of 1.77×10^{-2} mole L^{-1}, with the most abundant ions being Na, sulfate, and Cl. At W/R of 100 during alteration, the total dissolved solids are 2.4×10^{-2} mole L^{-1} with the most abundant ions being Na, S species, and Cl.

It is this fluid that could evaporate to form the observed sulfate minerals. This fluid, when compared

Table 3. Fluids forming clay minerals in rocks of Martian meteorite composition and rocks measured by the Mars Exploration rovers. Data from Bridges and Schwenzer (2012; Lafayette), Filiberto and Schwenzer (2013; Fastball), and Schwenzer and Kring (2009, 2013; LEW88516, Humphrey, Chassigny, Dhofar 378).

W/R 1000	Lafayette	Fastball	Humphrey	Chassigny	Dhofar 378	LEW 88516
Cl^-	1.67E-02	5.89E-02	5.87E-02	5.87E-02	5.87E-02	5.87E-02
HCO_3^-	1.68E-05	1.68E-05	1.68E-05	1.68E-05	1.68E-05	1.68E-05
S*	2.47E-03	2.28E-03	2.62E-03	1.14E-03	2.44E-03	1.46E-03
HPO_4^{2-}	2.13E-09	1.69E-10	1.29E-09	2.14E-12	1.25E-09	1.87E-10
K^+	1.08E-04	4.88E-05	2.12E-05	8.70E-06	3.61E-05	6.37E-06
Na^+	3.10E-04	7.58E-04	8.20E-04	4.13E-05	6.71E-04	1.74E-04
Mg^{2+}	7.42E-03	2.32E-02	2.29E-02	2.78E-02	2.16E-02	2.64E-02
Ca^{2+}	2.92E-03	3.42E-03	3.77E-03	2.59E-03	4.16E-03	3.16E-03
Al^{3+}	1.55E-09	5.45E-07	2.21E-10	5.41E-14	2.48E-10	3.48E-13
Fe**	1.90E-04	4.75E-03	4.87E-03	3.80E-06	5.59E-03	1.08E-03
SiO_2(aq)	1.29E-04	4.01E-05	4.89E-05	5.57E-05	4.91E-05	5.48E-05
W/R 100	Lafayette	Fastball	Humphrey	Chassigny	Dhofar 378	LEW 88516
Cl^-	1.67E-02	6.04E-02	5.85E-02	5.87E-02	5.84E-02	5.85E-02
HCO_3^-	1.68E-05	1.68E-05	1.68E-05	1.68E-05	1.68E-05	1.68E-05
S*	2.43E-03	2.35E-06	1.08E-03	2.78E-08	1.70E-03	1.61E-09
HPO_4^{2-}	3.43E-12	3.13E-14	9.38E-14	5.77E-13	1.74E-13	1.94E-13
K^+	1.08E-03	4.88E-04	2.12E-04	8.70E-05	3.61E-04	6.37E-05
Na^+	3.10E-03	7.58E-03	8.20E-03	4.13E-04	6.71E-03	1.74E-03
Mg^{2+}	2.13E-03	1.52E-02	1.15E-02	2.47E-02	8.58E-03	1.86E-02
Ca^{2+}	5.80E-03	1.04E-02	1.40E-02	3.43E-03	1.81E-02	9.11E-03
Al^{3+}	1.57E-09	4.42E-14	1.41E-13	1.54E-16	3.91E-12	7.78E-15
Fe**	7.04E-07	5.11E-06	2.41E-06	2.41E-04	6.17E-06	2.50E-05
SiO_2(aq)	1.28E-04	5.63E-05	5.62E-05	8.24E-06	5.53E-05	5.17E-05

*sum of all S species, **sum of all Fe in Fe species.

to those derived from whole-rock alteration or the alteration of the amorphous phase alone, is characterized by the lowest P and Al and the highest K concentrations. Fe, Ca, and Mg appear to be high, but not uniquely high, and Na and Si match the concentration range observed from the alteration of the suite of rocks modeled. The Gale crater fluids offer key elements to contribute to the habitability of the site (see Grotzinger et al. 2014), but factors beyond the fluids need to be considered for the full picture (Conrad 2014). In the Discussion section, we consider the Gale model fluids in the context of Martian starting materials, such as meteorites and MER rock compositions, and in the context of fluids derived from experiments with Martian analog starting compositions, as well as a variety of terrestrial fluids.

Evaporation of Gale crater Fluids

The observation of sulfate veins within the Yellowknife Bay units (McLennan et al. 2014; Nachon et al. 2014; Schroeder et al. 2015) indicates fluid movement into those fractures and subsequent increasing salinity to precipitate the salts. There are two processes which increase salt concentration in a brine: the removal of liquid H_2O via freezing or by evaporation. Both processes are similar in that they increase salinity and decrease water activity, which results in many of the same precipitates. However, detailed investigations (e.g., Marion et al. 2008; Fairén et al. 2009; Elsenousy et al. 2015; Toner et al. 2015) have shown that differences might exist, especially in detailed thermodynamic treatment of highly saline, perchlorate containing solutions, but also in the amount of constituents expected to precipitate from solution. We focus on evaporation here because the sulfates are found in vein-type deposits within a complex lake bed stratigraphic sequence providing evidence for repeated liquid water episodes punctuated by dry episodes (Grotzinger et al. 2014; Vaniman et al. 2014) open the possibility for such evaporation of fluids that are later diagenetic in relation to subsurface strata. We acknowledge that freezing cannot be excluded. Evaporation can occur in two ways: (1) in place, "batch" evaporation without water movement and (2) water movement and fractionation of the minerals during evaporation.

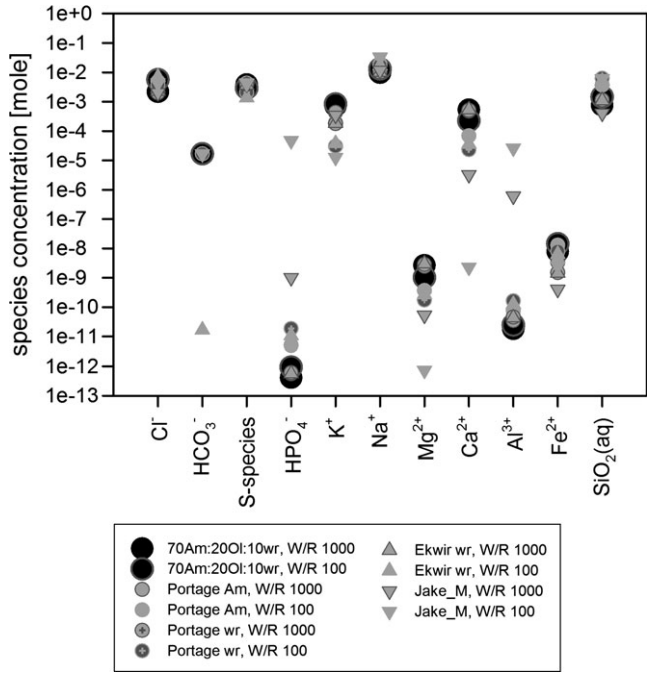

Fig. 3. Fluid compositions of diagenetic fluids forming clay minerals in a variety of Gale crater rocks. 70Am:20Ol:10wr is the fluid derived from incongruent dissolution of Portage soil, which has been found the best fit to form clay minerals as observed at Yellowknife Bay; see Bridges et al. (2015) for details. Data for rock compositions from Gellert et al. (2013), Morris et al. (2013, 2014), Stolper et al. (2013), Schmidt et al. (2014), and Vaniman et al. (2014), and see the 'Methods' section.

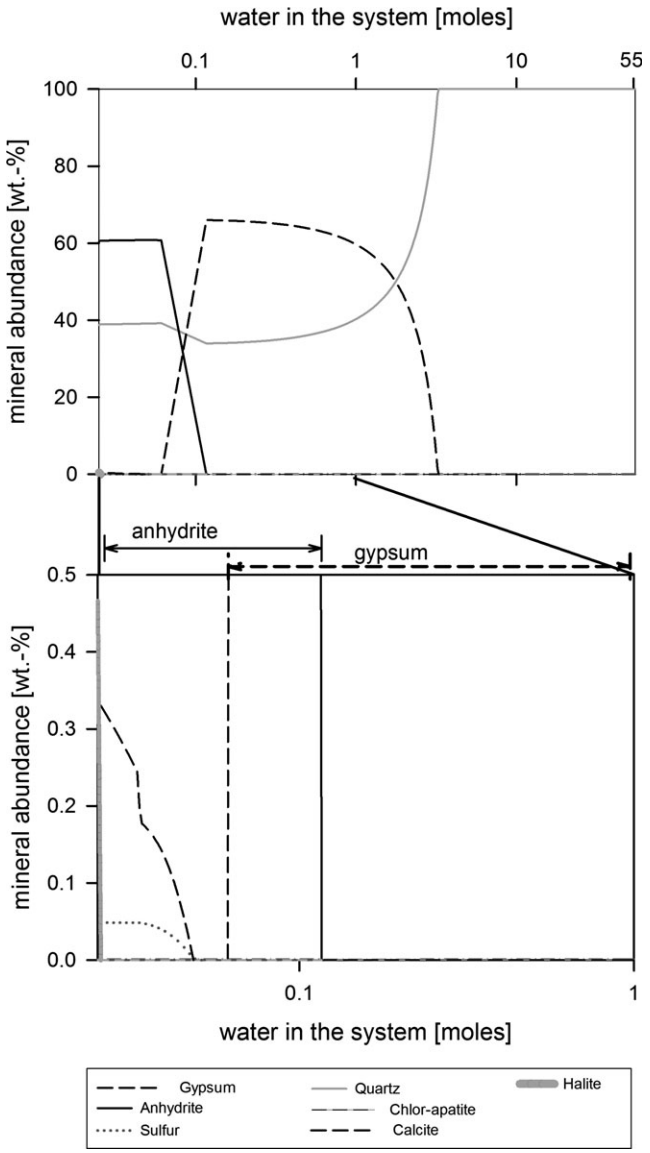

Fig. 4. Batch evaporation of the fluid deduced from the incongruent dissolution and precipitation of alteration phases of Portage soil (dissolving is the "mix" composition, which is 70% amorphous phase, 20% olivine, and 10% whole rock, fluid taken at W/R of 1000).

The required model for in-place evaporation is a "batch" water removal model (Fig. 4), which does not remove any precipitated minerals from the system, and allows already precipitated phases to re-react with the fluid. This unfractionated evaporation of the "mix" fluid composition at W/R 1000 results in a quartz (or amorphous silica, depending on kinetics) and sulfate-dominated precipitate, where the first mineral to precipitate is silica followed by gypsum, and with further increasing salinity, anhydrite in the models (Fig. 4, and see the Gypsum, Bassanite or Anhydrite? section for discussion on the hydration state of the sulfates). Trace amounts of apatite precipitate along with silica and gypsum at lower salinity. The precipitation of minor calcite, halite, and dawsonite occur when less than 0.5 moles water is left in the system.

In contrast, the fractionating model (Fig. 5) removes previously precipitated minerals out of the evaporating system. Fractionated precipitation from the "mix" fluid composition at W/R 1000 produces many of the same minerals as the batch model (Fig. 5), but in contrast to unfractionated precipitation, precipitation of the individual mineral species does not overlap significantly during the decrease in water in the system. In other words, a clear succession of quartz (or amorphous silica, depending on kinetics), sulfate, and sulfate + carbonates is observed. We note that in real evaporation scenarios, fractionation occurs when layers of minerals are deposited and are no longer in direct contact with the fluid anymore. However, in nature salinity changes (e.g., though period influx of fresh water) cause layering and mixing of the precipitates (e.g., Last 1989).

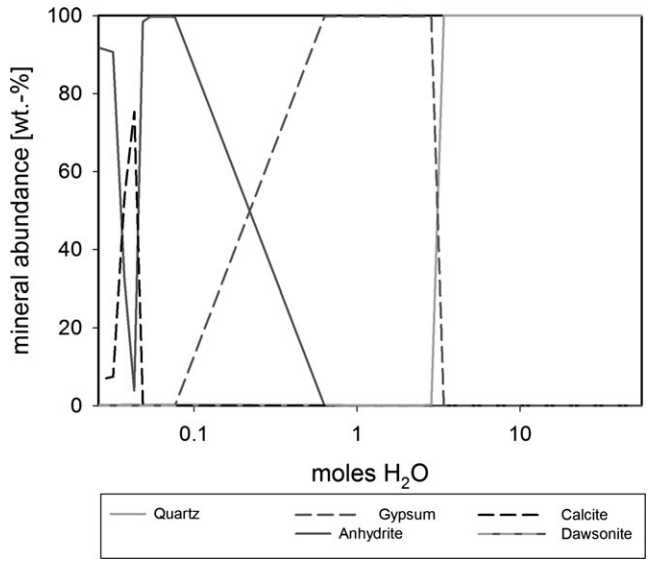

Fig. 5. Fractionated evaporation of the fluid deduced from the incongruent dissolution and precipitation of alteration phases of Portage soil (dissolving are 70% amorphous phase, 20% olivine, and 10% whole rock, fluid taken at W/R of 1000).

The total concentration of Ca and S species in the evaporating fluids is 5.3×10^{-4} mole L^{-1} at W/R 1000 and 2.25×10^{-4} mole L^{-1} at W/R 100; S species concentration varies at $3.5 \times 10^{-3} \pm 0.5 \times 10^{-3}$ mole L^{-1} between W/R of 1000 and 100. Thus, Ca concentration is the limiting factor for Ca-sulfate formation and a maximum of 5.3×10^{-4} mole L^{-1} (or 0.07 g of anhydrite from 1 kg of solution) can be precipitated. At W/R of 1000, this kg of solution contains 1 g of dissolved host rock. Thus, per g (or ~3–3.5 cm^3) of host rock 0.07 g of anhydrite (or 0.02 cm^3; assuming a density of 2.97 g cm^{-3}) could be formed. Given the abundance of veins and vesicle fillings in some areas at Yellowknife Bay, large-scale fluid movement or a concentration process may have been required.

DISCUSSION

We structure this discussion into two main sections: the fluids during alteration mineral formation (Fluids) and the evaporation of such fluids (Evaporation). In both sections, we present comparisons and terrestrial analogs.

Fluids

Gale Fluids in Comparison to Other Mars Fluids Associated with SNC Parent Rocks and Viking, Pathfinder, and MER Landing Sites

Martian fluid compositions obtained from clay-forming models exist for a variety of meteorites and also for rocks measured by the MER rovers (Table 2). To date, the most precise modeling of SNC parent rock alteration has been obtained for nakhlite Martian meteorite alteration, especially for the carbonate–smectite–gel veins in Lafayette (Bridges and Schwenzer 2012). The precision of the model is critically dependent on the information available about the system. About 1% of the meteorite is taken up by alteration veins (Changela and Bridges 2010), which mainly consist of Ca-rich siderite (Bridges and Grady 2000; Bridges et al. 2001), phyllosilicate (ferric saponite and serpentine; Changela and Bridges 2010; Hicks et al. 2014), and a ferric gel of saponitic composition (Changela and Bridges 2010). These observations led to a model of incongruent Lafayette dissolution—70% olivine, 20% bulk rock, 10% mesostasis. This dissolving composition causes Ca-siderite precipitation at high temperatures ($150 \leq T \leq 200$ °C) and a residue of Si, Na, and K in the fluid, which is thus added to the elements available from the dissolving rock during smectite precipitation. The latter occurs at ~50 °C and pH 9. For comparison with all other fluids considered here, the fluid during the smectite precipitating reaction is reported here at W/R of 1000 and 100 (Table 3). More details of the fluid composition are given in Bridges and Schwenzer (2012).

Alteration of the oldest known Martian meteorite, the carbonate-bearing ALH 84001, has also been modeled. The incoming fluid was a dilute brine, as deduced from low-temperature fluids that vent at the Deccan Traps (Minissale et al. 2000; Schwenzer and Kring 2009). In addition, we compare our results to data for ALH 84001 from Melwani Daswani et al. (2016), who reacted bulk ALH 84001 host rock in a 1D flow model. Total dissolved solids range from 1.3×10^{-2} to 4.4×10^{-2} mole L^{-1} between W/R 1000 and 100. Apart from carbon species, which dominate in CO_2-bearing models, the following elements are important carriers of the salinity: at W/R = 1000, the most abundant species in solution are Mg, Si, and Ca (molalities: 6.2×10^{-3}, 1.7×10^{-3}, and 3.2×10^{-4} mol kg^{-1} H_2O, respectively). At W/R = 100, the most abundant species are Mg, Na, and Si (molalities: 3.8×10^{-3}, 3.4×10^{-4}, and 1.2×10^{-4} mol kg^{-1} H_2O, respectively). For details on fluids that could be associated with alteration of Martian rocks from the MER rovers and from shergottite and chassignite type compositions, see Filiberto and Schwenzer (2013; Fastball) and Schwenzer and Kring (2009, 2013; LEW88516, Humphrey, Chassigny, Dhofar 378).

On a triangular plot of (Na+K)—(Fe+Mg+Ca)—SiO_2, which facilitates the separation of key elements based on their solubility and precipitation properties, the notable difference between Gale fluids and other

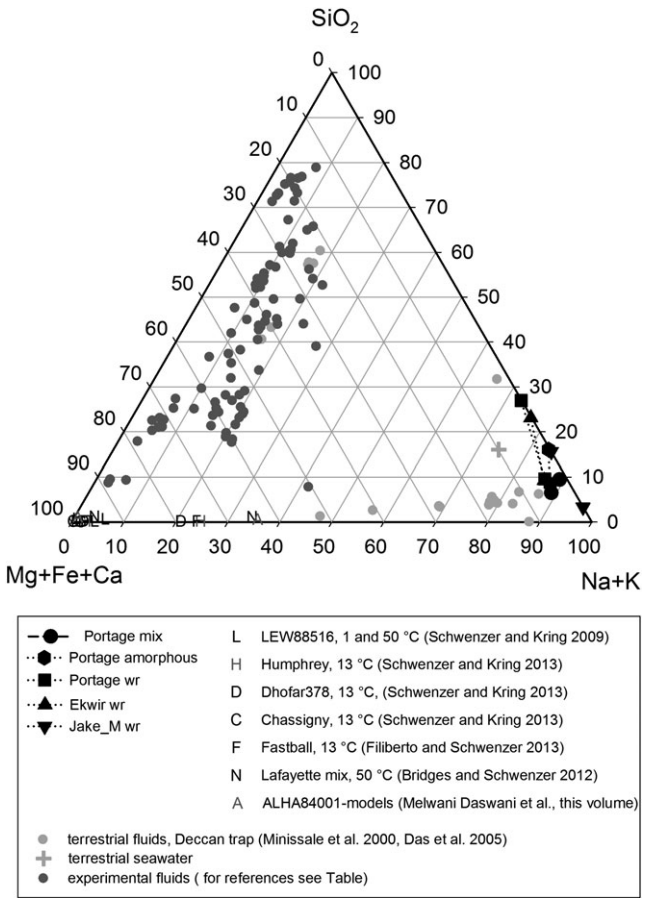

Fig. 6. Ternary plot showing the relationship between the dissolved alkali metals, the dissolved alkaline earth metals (plus Fe), and dissolved silica. We include Fe with the alkaline Earth elements because it frequently occupies the same crystallographic sites in host rock and alteration minerals. We note, however, that Fe concentrations are generally low in solution because of its low solubility in the presence of oxygen. In most modeling and experimental fluids, the partial pressure of oxygen is high enough for Fe-oxides or hydroxides to form. For references of the experimental fluids, see Table 2. Note that some of the Deccan Trap fluids fall into the alkali-rich corner of the plot, while others are particularly alkali-poor compared to their relative content in alkaline earths and silica.

Martian fluids is the higher relative concentrations in alkali elements—and in some cases dissolved silica (Fig. 6). This is consistent with the higher abundance of those elements in many of the Gale rock compositions, especially for the alkali elements, which mainly stay in solution at the W/R plotted here. Investigating the elemental relationships in more detail (Fig. 7), it becomes clear that it is Na that causes the observed difference, while K concentrations of the fluids derived from two rock groups are more similar. Al and S species concentrations are similar in both groups. Fe, Mg, and Ca are up to orders of magnitude higher in the meteorite-derived fluids than in Gale crater fluids, with especially Mg being very low compared to any other Martian fluid composition. Note that the amorphous phase in Portage soil as calculated by Morris et al. (2013, 2014) is low in Mg. The Mg-poor nature of the amorphous phase is reflected in all Gale crater model fluids that use this component and is most prominent when the amorphous component contributes a large share of the dissolving host rock to reflect its high reactivity. Therefore, dominance of the amorphous component during incongruent dissolution of the host rock causes a Mg-poor system. The Mg depletion is further enhanced by the formation of Mg-bearing clay minerals.

Localizing the Gale fluids in a diagram $Mg/(Na_2+Mg)$ versus $SO_4/(Cl_2+SO_4)$ (Hardie and Eugster 1970), the Mg deficiency becomes even clearer, since the $Mg/(Na_2+Mg)$ varies between 44×10^{-12} and 0.5×10^{-6}, while the $SO_4/(Cl_2+SO_4)$ varies between 0.28 and 0.80. Thus, Mg concentrations are minimal and the only variation is in the anions. The species relationships in the dilute brine suggest the formation of Na-sulfates, more specifically thenardite (Na_2SO_4) and mirabilite ($Na_2SO_4 \times 10\ H_2O$). Note that mirabilite is not stable under dry conditions, and the amount precipitated might be below the detection limits of CheMin, especially if vein material is mixed in with other material, as is the case in the Cumberland and John Klein drill holes (Vaniman et al. 2014) upon sufficient concentration of the solution during evaporation. We will discuss evaporation in the Evaporation section, but note here that the S species precipitating at higher salinities is native S. The difference is a result of the system's redox conditions, which we are currently exploring in detail (Schwenzer et al. 2016a, 2016b). King et al. (2004) used the diagram by Hardie and Eugster (1970) to localize the Viking and Pathfinder soils, which plot above 0.7 in $Mg/(Na_2+Mg)$ and above 0.8 in the $SO_4/(Cl_2+SO_4)$, and are, therefore, in the $MgSO_4$ field. The Portage soil from Gale crater has a $Mg/(Na_2+Mg)$ of 0.55 and $SO_4/(Cl_2+SO_4)$ of 0.64 and thus plots considerably further to the Na_2Cl_2 corner of the diagram than any other Martian composition available to King et al. (2004) for their comparison. If incongruent dissolution is taken into account, and the amorphous phase contributes 70% of the dissolving rock (with 20% ol and 10% wr), the $Mg/(Na_2+Mg)$ is 0.67 and $SO_4/(Cl_2+SO_4)$ is 0.63, reflecting the increase in both MgO and Na_2O in the dissolving mixture. The dissolving mixture is still much closer to the Na_2O endmember than Viking and Pathfinder rock compositions (King et al. 2004). This underlines the difference between Gale and other Martian compositions especially in the concentrations of more soluble elements.

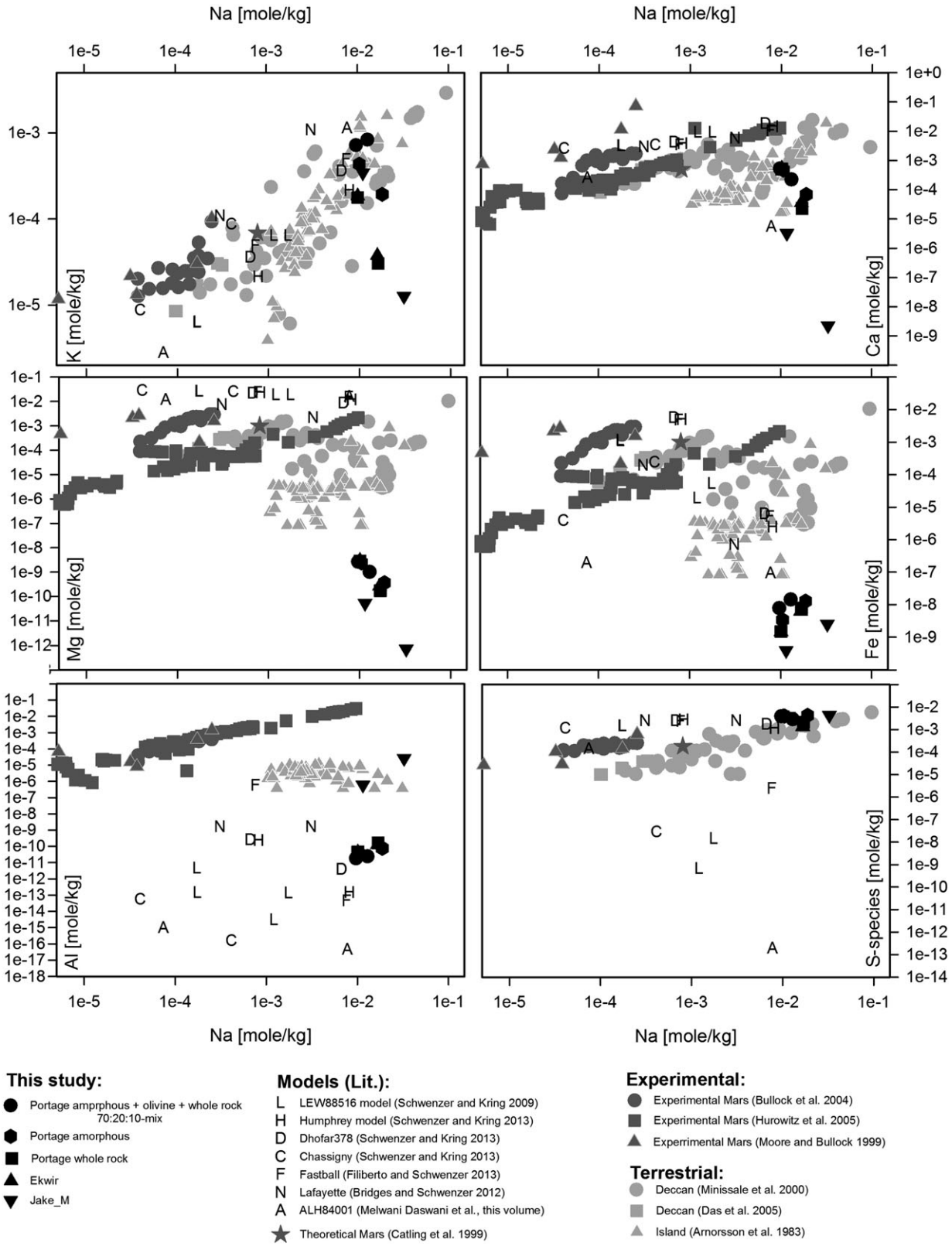

Fig. 7. Element concentrations in solution. Data for Gale crater models (black), model fluids from other locations and meteorites (letters), experimental Martian fluids (dark gray), and terrestrial fluids (light gray). Deccan Tap fluids are represented by the light gray circles and squares. Terrestrial seawater is not shown because of its higher overall concentration, especially in Na.

The clay-forming fluids have much lower Mg/Ca and Fe/Ca molar ratios than carbonate forming fluids, e.g., as modeled by Niles et al. (2009). The Mg/Ca ratio is orders of magnitude lower in Jake_M fluids than in the ALH 84001-derived fluids, whereas the Fe/Ca ratio is similar. In contrast, Portage mix fluids have orders of magnitude lower ratios for both Fe/Ca and Mg/Ca due to the formation of Fe and Mg clays, but temperature effects and the presence of CO_2 in the ALH 84001 models account for a significant proportion of the differences because Mg/Ca and Fe/Ca decrease with decreasing CO_2 partial pressure (Niles et al. 2009). For Gale, the absence of carbonates in the veins and mudstones (Nachon et al. 2014; Vaniman et al. 2014) and the composition of the clays (e.g., Bridges and Schwenzer 2012; Melwani Daswani et al. 2016) indicate that the system was not in contact with the Martian atmosphere at the time of vein formation, and therefore, carbonate precipitation does not need to be considered here.

Gale Fluids in Comparison to Mars Experimental Fluids

Comparison of the Gale crater fluids to Martian experimental brines returns many of the same observations as the previous comparison to the modeled fluids, except in the (Na+K)–(SiO_2)–(Mg+Fe+Ca)–space. The reason for this discrepancy is the higher Na+K value of the modeled brines. This is likely due to the combination of two effects. (1) The models do not take adsorbed or exchangeable clay interlayer cations into account, but experimental precipitates will contain such elements. (2) The experiments are not always adapted to the exact Martian rock compositions; e.g., Bullock et al. (2004) use an approximate Martian rock composition, which has about half the FeO concentration in their starting mineral mixture than in the Zagami shergottite Martian meteorite they use for comparison. As seen in this study when comparing the Jake_M derived fluids to other compositions, the fluid composition is sensitive to such changes. While this does not compromise the Bullock et al. (2004) findings, because soils of such composition had been found elsewhere on Mars, this demonstrates the sensitivity of the results to the actual host rock composition. In addition, their experiments were carried out under CO_2 atmosphere. Recently, we modeled a similar composition under similar conditions as the Bullock et al. (2004) experiments and found the Na-bearing zeolite stilbite and Na-nontronite form (Schwenzer et al. 2016a, 2016b), which is in agreement with similar models for CO_2-rich alteration of the Nili Fossae region (Van Berk and Fu 2011). This adds evidence that the Gale crater mudstones and their accompanying fluids formed in the subsurface with no, or very limited, contact with the atmosphere because the CO_2-poor Gale crater models return Mg-nontronite, chlorite, and serpentine, matching the compositions of the clays observed at Yellowknife Bay (Bridges et al. 2015).

In addition, experimental fluids might be different because of incongruent dissolution. We have argued previously that initial incongruent olivine dissolution could have favored Mg-rich fluids and formed the raised ridges (see Bridges et al. 2015; Léveillé et al. 2014). Experimental results on Martian composition, which discuss incongruent dissolution, found changes in several key elemental ratios and an increase in SiO_2 concentration over time in all batch reactions and one of the flow-through experiments (Hurowitz et al. 2005). Other important details include pH, which influences the dissolution behavior of the host rock minerals (see, e.g., Zolotov and Mironenko 2007; Gudbrandsson et al. 2011). Some of the experimental conditions were set to be acidic (e.g., Hurowitz et al. 2006), but the pH evolves to neutral and alkaline values over the course of the models of this study. This pH evolution is similar to the experimental observations of Tosca et al. (2004), who find that dissolution of basaltic material neutralizes solutions to be assumed for acidic weathering on Mars forming secondary minerals such as Fe-oxides and silica, not Fe-smectites. Therefore, the observation of Fe-smectite at Gale crater, which can be matched with model reactions of neutral to alkaline fluids (Bridges et al. 2015), supports the conclusion that the fluids modeled here are a potential pore fluid resulting from the diagenesis at Gale crater. The presence of clays—among other mineralogical evidence—points to diagenetic, groundwater-type fluids and not reactions with an acidic or CO_2-saturated brine. Early precipitation of Mg-rich clays resulted in a Mg depletion in the fluid.

Gale Fluids in Comparison to Selected Terrestrial Fluids

Terrestrial fluids in basaltic host rocks are mostly also influenced by the presence of seawater, e.g., at the Mid Ocean Ridges, and on Iceland and Hawaii. Terrestrial fluids venting from a large volume of basaltic rocks without modern seawater influence can be found in the Deccan Trap units. These span a similar but wider chemical-compositional range than the Gale crater fluids in the Na+K–SiO_2–Mg+Fe+Ca–space (Fig. 6; Minissale et al. 2000; Das and Krishnaswami 2007). They are especially similar in the Na, K, Ca, and S species concentrations. Note that no Al data are reported for the Deccan Traps. Mg and Fe are notably lower in the Gale model fluids, confirming the low Mg concentrations observed in comparison to Martian experimental and modeled fluids (see the Gale Fluids in Comparison to Mars Experimental Fluids and Gale Fluids in

Comparison to Selected Terrestrial Fluids sections), but also indicating that Fe measurements in real fluids are often higher than in model fluids due to complexation of the otherwise very insoluble Fe with organic salts in the natural fluid. The Icelandic fluids shown in Fig. 7 are selected for their low Na concentration as a proxy for the absence of seawater. The selected fluids are similar to the Deccan fluids in Na and K abundances, but are intermediate in their Fe and Mg concentrations between the Deccan and Gale fluids.

Evaporation

Next, we discuss the evaporation of the fluid derived from the Portage mix alteration. We start the section with the discussion of the different sulfate hydration states (gypsum, bassanite, anhydrite) during precipitation and their stability in today's Martian atmosphere. We next discuss the results of our evaporation models and compare them to other model results from the literature and evaporation experiments with Martian analog compositions. We then consider terrestrial fluids and focus our analog discussion on Triassic mudstones with gypsum veins from the Mercia Mudstone Group at Watchet Bay, Southwest UK.

Gypsum, Bassanite, or Anhydrite?

First, we address the question of how the hydration state of minerals measured by CheMin on Mars might relate to the initial precipitate, because hydration and dehydration commonly occur in those minerals, after the formation of the initial precipitate.

Traditionally, experimental data at low temperature favor gypsum precipitation, but anhydrite has been predicted in highly concentrated solutions at temperatures as low as 18 °C (Ossorio et al. 2014). However, a conundrum existed in that laboratory experiments resulted in gypsum precipitation, whereas in nature, anhydrite would be observed. Recent studies (Van Driessche et al. 2012; Ossorio et al. 2014) suggest that the formation pathway is more complex. Gypsum is the first precipitate at early stages from most solutions, but maturation to anhydrite in contact with the more saline solutions occurs on a time scale of months to years depending on temperature (Ossorio et al. 2014). In addition, gypsum and bassanite are subject to dehydration under low water partial pressure conditions. For example, Carbone et al. (2008) investigated hydrated sulfate behavior under reduced pressure (1 mbar) and at a temperature range from ~40 °C to ~80 °C and found that gypsum dehydrates to γ-anhydrite in a one-step reaction, but that this γ-anhydrite (in contrast to the insoluble β-anhydrite) readily re-hydrates to bassanite. We note that the observed bassanite on Mars (Rapin et al. 2015) could be a dehydration product forming under the current Martian conditions. On sol 182 (John Klein drilling; Ls 260.7, Southern hemisphere spring), the pressure varied between P_{max} 965 Pa and P_{min} 864 Pa, the air temperature between T_{max} 265 K and T_{min} 207 K, and the surface temperature (T_g = surface brightness temperature) between $T_{g\ max}$ of 275 K and $T_{g\ min}$ of 203 K. This results in a maximum of relative humidity of RHa = 10.970% and RHg = 16.370%. On sol 292 (Cumberland drill hole, Ls 321, Southern hemisphere summer), the pressure varied between P_{max} 904.43 Pa and P_{min} 795.36 Pa and the air temperature between T_{max} 262 K and T_{min} 205 K. The surface temperature ranged from $T_{g\ max}$ of 267 K to $T_{g\ min}$ of 205 K, resulting in a relative humidity of RHa = 9.810% and RHg = 17.440%. From these measured T and pressure conditions at the Gale surface, the maximum water activity at 15 cm depth can be modeled and ranges from RH_15 cm 0.252% (Cumberland drill sol 292) to RH_15 cm 0.295% (John Klein drill sol 180).

Robertson and Bish (2013) showed that subaerial dehydration of gypsum is slow under current Martian atmospheric conditions, depends on particle size and temperature, and leads to bassanite. Soluble anhydrite rehydrates to bassanite even under extreme conditions of low temperature (−15 °C) and less than 1% relative humidity. The next step—rehydration of bassanite to gypsum—is only possible in the presence of ice under current Martian atmospheric conditions (Vaniman et al. 2009; Robertson and Bish 2013). Note that in the experiment, dehydration occurred within the 48 h observation time frame in <45 μm grains and at 355 K (Robertson and Bish 2013). This is relevant when interpreting the drilled sample results because the grain size of the sieved fraction admitted into CheMin is <150 μm (e.g., Vaniman et al. 2014). Therefore, to compare the model results to Gale crater observations introduces the complication that the originally precipitated mineral might have changed hydration state between formation and observation. However, ChemCam has sampled calcium sulfate veins at numerous locations along the rover traverse and is able to instantly estimate the hydration level. It was found to be mostly consistent with bassanite, which likely comes from the dehydration of gypsum, near the surface or with some degree of burial (Rapin et al. 2015). In the following, we give gypsum and anhydrite as calculated, because the transition is a salinity indicator in the model, but note that this might be a simplification and/or the hydration/dehydration effects in the current low pressure, arid environment might have led to alteration of gypsum to bassanite (Rapin et al. 2015).

Precipitates

When deciphering formation conditions of the veins at Gale crater, an important factor to consider is the purity of the sulfate as several factors will influence the nature of the precipitate. The Gale crater fluid (Table 1) is derived from circum-neutral alteration of the basaltic host rock (Bridges et al. 2015) and thus contains more than just the building blocks for Ca-sulfate precipitation. Most notably, the Si concentration is such that any change in thermochemical conditions leads to silica (amorphous or quartz) precipitation (Figs. 4 and 5). This is supported by previous models of Martian brines (McAdam et al. 2008), but it contrasts to acid alteration models starting with fluids supersaturated in jarosite (Marion et al. 2008), a mineral observed upsection from the Yellowknife Bay area in minor amounts (Vaniman et al. 2015), but not at the Cumberland and John Klein Drill sites (Vaniman et al. 2014). Thus, the evaporation sequence of silica, gypsum/anhydrite to easily soluble salts is found from the groundwater-type fluids in the Gale area, and this finding is supported by studies on Martian compositions in different geographic locations on Mars.

The nature of the atmosphere—ancient Mars versus present day Mars—further controls the evaporation conditions. This was investigated experimentally by Moore et al. (2010), showing that, under CO_2-rich, "acidic" atmospheric conditions with volcanic gas additions (CO_2 atmosphere with traces of SO_2, N_2O, HCl; Moore et al. 2010) equivalent to ancient Mars, evaporites from a Mars analog brine are dominated by magnesium sulfates, whereas in precipitates under conditions more equivalent to present day Mars atmosphere (95.50% CO_2, 2.70% N_2, 1.60% Ar, 0.13% 0_2, and 0.07% CO; Moore and Bullock 1999), Ca-sulfates dominate. Note that one major difference is the pH of the fluid, which is likely buffered by the high CO_2 concentrations and influenced by the SO_2 in the "ancient atmosphere" conditions. Sulfates are generally formed in acid-driven, S-bearing Mars analog alteration (e.g., Hurowitz et al. 2005; Tosca and McLennan 2009), whereas CO_2-dominated, S-poor acidic conditions cause carbonate precipitation (Niles et al. 2009). Since Ca-sulfates, but no Mg-sulfates and no carbonates, are observed in the veins at the Yellowknife Bay site, this is once again indicative of the subsurface, CO_2-poor, neutral to alkaline nature of the fluids.

More generally, a Martian evaporation sequence is expected to contain silica and siderite, which might undergo cycles in deposition, similar to what is observed in terrestrial evaporites (Catling 1999). The siderite is followed by magnesite, then gypsum (Catling 1999). After sulfate formation, the more soluble salts will form (e.g., Catling 1999). Na-sulfate is one option, as seen in the diagram by Hardie and Eugster (1970; see the Gale Fluids in Comparison to Other Mars Fluids Associated with SNC Parent Rocks and Viking, Pathfinder, and MER Landing Sites section), with respect to halite plus sulfur (Fig. 4) depending on the redox state of the system. In the nakhlite Martian meteorites, halite has been observed (Bridges et al. 2001), and at the Phoenix landing site, a complex interplay of sulfate and perchlorate formation might exist (see, e.g., Toner et al. [2015] for a discussion and model). We consider the high salinity brines beyond the scope of this article but an interesting separate study, because only sulfate has been observed in the veins, while oxychlorine minerals (e.g., perchlorates or chlorates; e.g., Glavin et al. 2013; Leshin et al. 2013; Ming et al. 2014) and other soluble salts (nitrates, Stern et al. 2015; halite, Vaniman et al. 2014) have been detected in the rocks and soils. On a technical note, high ionic strength fluids ($i > 5$; which occurs when ~0.06 mole H_2O is left in the system) cannot be modeled accurately with the code used here and thus would require a separate set of considerations, techniques, and models.

In summary, the mineral sequence modeled to precipitate from the fluid appears to be a sequence of evaporation phases commonly found in such environments, but the Mg species are absent or only present as trace phases in the sulfate veins. This leads to the conclusion that the pH of the fluids was circumneutral.

Another important consideration for the interpretation of the veins at Yellowknife Bay is the fact that they appear to be predominantly pure bassanite (Rapin et al. 2015) with no silica-rich rim or high trace element content (Nachon et al. 2014). This is contrary to the models, where an in place evaporating fluid would still contain silica, and thus a silica polymorph is expected to be observed. The formation model, therefore, requires a process to spatially separate the sulfate from the early precipitation of silica and the later precipitation of more soluble salts. One option is fractionated precipitation as in our second model (Fig. 5) of a fluid moving along a fracture. Another option is re-dissolution of an initially mixed evaporite layer, which we discuss in the Evidence for Re-dissolution section, after we have compared the Gale vein-type sulfates to other occurrences of sulfates on Mars.

Sulfates Elsewhere on Mars

The Gale crater site is neither the first place on Mars where sulfates have been found nor the first place for which evaporation has been suggested as the main formation process (see Gaillard et al. [2013] for a review). Sulfates have been found in the nakhlite Martian meteorites (Bridges and Grady 2000), by the

THEMIS (e.g., Vaniman et al. 2004), OMEGA (e.g., Bibring et al. 2005, 2006; Gendrin et al. 2005; Langevin et al. 2005), and CRISM (e.g., Thomson et al. [2011] for Gale; Carter et al. [2013] and Gaillard et al. [2013] for review) orbiter instrument observations and found inferred through landed spacecraft measurements from Viking (Clark et al. 1976), to Sojourner (Bell et al. 2000), Phoenix (Kounaves et al. 2010), and MER (e.g., Rieder et al. 2004; McLennan et al. 2005; Gellert et al. 2006; Wang et al. 2006). All landed missions have all found high S concentrations in Martian soils and some rocks.

While many of the observed occurrences either lack outcrop-scale geological context, because they are orbital data, or are determinations of sulfates in soils, the MER rover Opportunity has found vein-type sulfate deposits at Endeavour Crater (Squyres et al. 2012; Arvidson et al. 2014), which we will use here as a point of comparison. Endeavour Crater is a ~22 km diameter crater. The MER Opportunity rover investigated layered strata around its rim. The lowest (and oldest) investigated layer is the Matijevic formation, which is interpreted to be a phyllosilicate-bearing, partially spherule-rich rock type. On top of the Matijevic formation lies the Shoemaker formation, which comprises a potential thicker layer consisting of poorly sorted clasts with little matrix, above which are impact breccias containing dark angular clasts and a fine-grained soft matrix. The rocks show geochemical signs of hydrothermal alteration (Squyres et al. 2012; Arvidson et al. 2014). On top of the impact sequence, darker, granular sedimentary rocks of the Grasberg formation are observed, which are themselves overlain by the sulfate-rich sediments of the Burns formation (Grotzinger et al. 2005). Both the Matijevic and Shoemaker formation rocks are cut by gypsum veins, which could have been formed by impact-related fluid movements (Squyres et al. 2012; Arvidson et al. 2014). Thus, the area investigated at Endeavour Crater reveals a complex sequence of clay formation, potentially postimpact hydrous alteration with vein formation, and finally acidic alteration at the Burns formation (Grotzinger et al. 2005; Arvidson et al. 2014). The interpretation of low temperature, potentially distal to the main heat source in space and/or time, impact-generated hydrothermal formation for the veins at Endeavour Crater (Squyres et al. 2012; Arvidson et al. 2014) is consistent with hydrocode models that locate the main activity (steam production, main fluid upwelling) in the center of relatively small (30 km diameter in the hydrocode simulation) craters (Abramov and Kring 2005). We note that the occurrence of the veins in postimpact sediments has a striking similarity between Endeavour and Gale crater Ca-sulfate veins. However, there are differences, too, in that the Gale crater rocks, in which the veins occur, lack signs of high-temperature hydrothermal activity and thus could potentially be separated in time from crater formation (Grotzinger et al. 2014). While Endeavour Crater strata are impact related, or interpreted as sediments sourced from the impact rocks, the sediments in Gale are widely accepted as lake bed sediments. The diagenesis of the earliest sediments, including vein formation, could still be supported by postimpact heat because craters of the size of Gale have longer lifetimes than small craters such as Endeavour. Abramov and Kring (2005) show that at about 20,000 yr after the impact, the melt sheet of a 180 km diameter crater would have cooled sufficiently to have completely crystallized and become permeable. Subsequently, this would allow for intense and increasing fluid circulation, which could affect overlying lake bed sediments that might already be in place. Terrestrial evidence for early lake bed sedimentation affected by the postimpact hydrothermal activity in the underground comes from the much smaller (~24 km diameter) Boltysh impact crater, where a postimpact temperature rise of up to 40 °C has been observed in the lake sediments (Watson et al. 2010; Williams et al. 2013a, 2013b). This demonstrates that the heating of early lake sediments from the underlying impact rocks is a potential factor in sediment diagenesis and fluid movements in the immediate postimpact history of a crater. While the Yellowknife Bay sequence might be too young compared to the age of the impact, underlying strata could contain relevant element enrichments, which are available for later mobilization. Relevant fluid movements are also possible through compaction, as the next analog demonstrates.

Evidence for Re-Dissolution

Summarizing the observations in the Precipitates and Sulfates Elsewhere on Mars sections shows that the Gale sulfates are vein-type, postsedimentation, and chemically pure. If a groundwater-type fluid leaching the wallrocks were to precipitate its ionic load without fractionation or refinement, a "dirty sulfate" would be expected (Figs. 4 and 5). We assume that the sulfate occurrences in soils all across Mars might be of impure nature and a result of batch precipitation. Veins at Endeavour Crater occur within impact strata and are likely postimpact hydrothermal, which implies a high-temperature origin. In contrast, the Gale crater sulfates occur in veins within sedimentary sequences, and those sedimentary sequences are widely believed to have been altered diagenetically (Grotzinger et al. 2014; Bridges et al. 2015). Therefore, the fluid precipitating the Gale crater veins is likely different from fluids precipitating sulfate into soils or at the Endeavour Crater rim. We

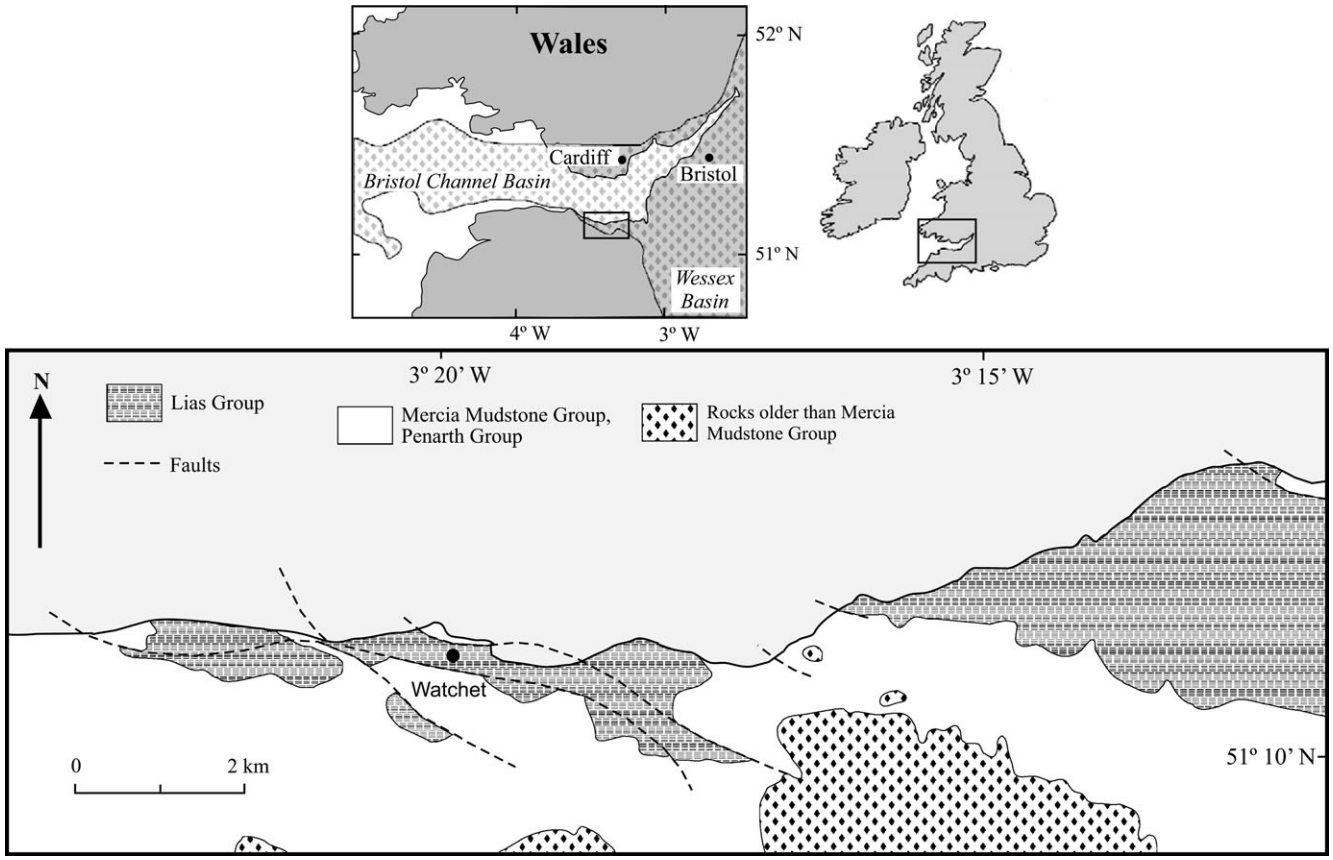

Fig. 8. Simplified geological map of Watchet and surrounding area geology in southwest UK. The Watchet cliffs and foreshore are composed of the Upper Triassic Mercia Mudstone group, which includes the diagenetic sulfate veins which are the subject of this article. Lias sediments are Lower Jurassic marine sediments that stratigraphically overly the MMG. Map based on Hounslow et al. (2004).

propose a two-step model with an initial fluid evaporation causing a "dirty sulfate" layer, or similar precipitation, within a sediment. This layer is likely below the formations so far investigated by the Curiosity Rover and buried. Upon burial, the sulfate could have been leached, leaving behind the less soluble phases and precipitating pure Ca-sulfate in the veins as observed.

Watchet Bay Terrestrial Analog: Geologic Similarities Between Gale crater, Mars, and the Mercia Mudstone Group, Watchet Bay, Upper Triassic, UK

The outcrops of 200 Myr Upper Triassic (Rhaetian) mudstones of the Somerset Coast, SW UK (Fig. 8) have analogous characteristics to the rocks at Yellowknife Bay. Cliff and foreshore outcrops along this coastline in SW England provide an almost continuous exposure, up to 67 m thick, of Upper Triassic and Lower Jurassic strata (Hounslow et al. 2004), which formed during Mesozoic extension of the Bristol Channel basin (Peacock and Sanderson 1999). Paleontological and lithological evidence shows the transition from continental playa–lacustrine environments, represented by the Mercia Mudstone Group in the Wessex Basin (as at Watchet Bay), to fully marine conditions represented by the overlying Jurassic (Lias) Group (Hounslow et al. 2004; Howard et al. 2008; Talbot et al. 1994; Warrington et al. 1995) (Fig. 9). Talbot et al. (1994) suggested that the red and gray mudstones and siltstones in the Mercia Mudstone Group (MMG) are of mixed floodplain and playa origin. According to Talbot et al. (1994), these MMG sediments accumulated in a low-relief interior basin flanked by subdued uplands of Upper Paleozoic sediments. The environment was principally a monotonous clay plain, which during humid periods and—following rains—contained shallow, freshwater to saline lakes.

The dominant evaporite mineral is gypsum, which occurs at distinct horizons, often as nodular aggregates as much as 30 cm in diameter with a chicken-wire texture. Veins and sheets of fibrous gypsum, in places parallel to and, elsewhere, cross-cutting the sedimentary bedding, are also prominent at some horizons in the cliff faces (Fig. 9) (Philipp 2008). In a study of the

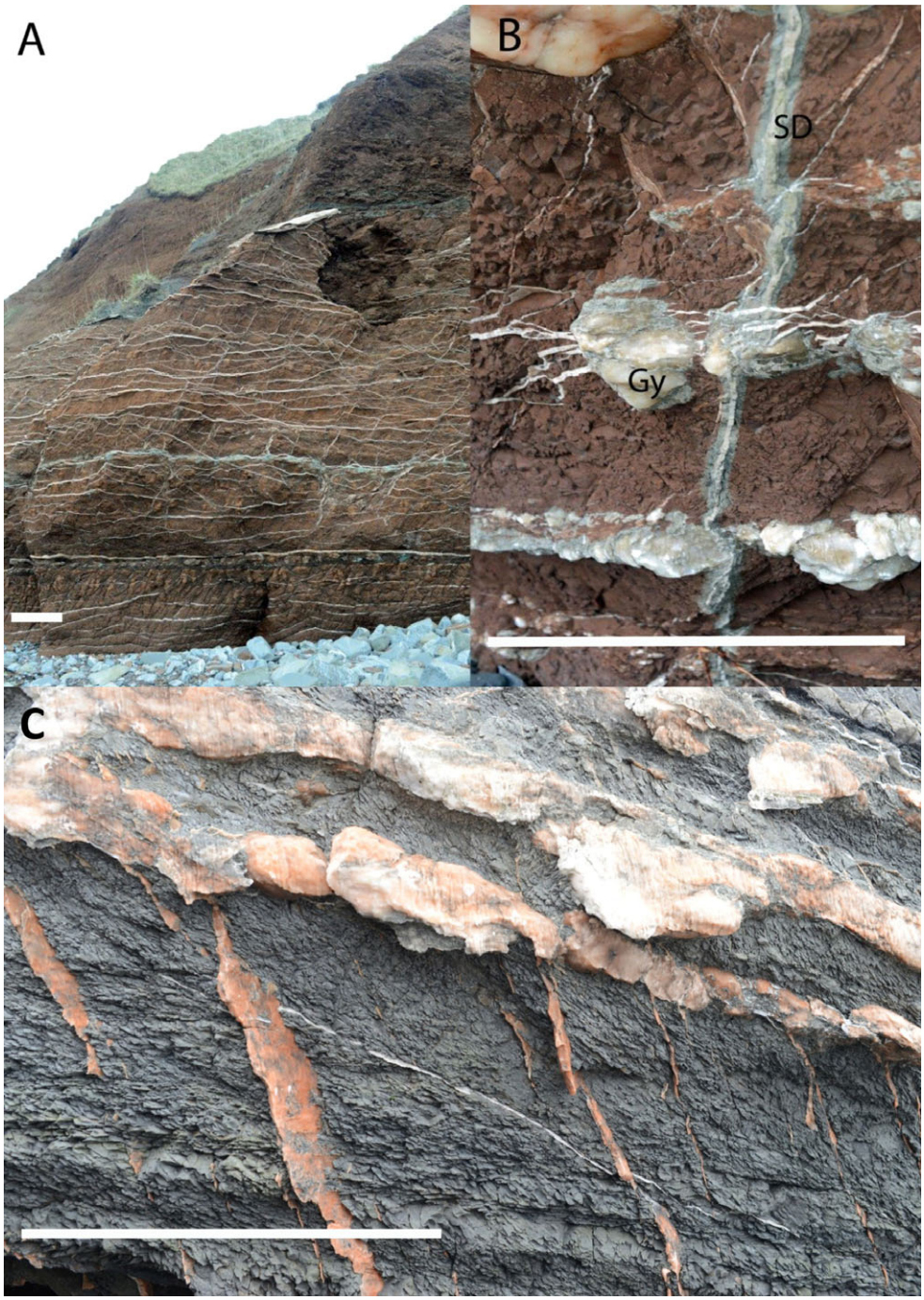

Fig. 9. Watchet Bay cliff outcrops on the N. Somerset coast, UK (51°10′59″N, 3°20′10.7″W). These outcrops consist of Upper Triassic sediments from the Mercia Mudstone Group thought to have formed in a mixed floodplain and playa origin environment (Talbot et al. 1994). A) This cliff outcrop contains nodular sulfate and clay mixtures toward the base (arrowed) and pure gypsum veins in the mid part of the cliff. Cliff height 30 m. Scale bar is 1 m. B) White gypsum veins derived by partial dissolution of sulfate-rich deposits formed by near-surface evaporation. SD sandstone dyke, Gy and clay gypsum nodule. Scale bar is 0.5 m. C) Pure gypsum veins (some with orange coloration) in gray mudstone member of Watchet Triassic mudstone. Scale bar is 0.25 m.

Mercia Mudstone Group, and comparing it to a range of recent Australian playas, Talbot et al. (1994) demonstrated that the Watchet sulfate-rich layers in the mudstone are diagenetic, probably formed from saline groundwaters in continental evaporitic mudflats. This can be envisaged as occurring during arid periods when the pore water would have become very saline, e.g., see Schreiber and el Tabakh (2000). A modern analog for

the bulk of the MMG is shown by muddy, ephemeral flood plains of the sort that cover vast areas of the interior of eastern Australia (Talbot et al. 1994).

Other features at Watchet, notably sandstone dykes, show similarities to Yellowknife Bay (Grotzinger et al. 2014), and since its identification as a Mars analog, the site has been used as a testbed for spacecraft instrument development (Turner et al. 2013), and compared to Gale crater veins for its hydrofracturing characteristics (Schieber et al. 2013; Nachon et al. 2014). Most important is the analogy in the sulfate compositions (Schwenzer et al. 2014; this study). This similarity gives rise to the question: Might an evaporite layer have been formed by precipitation from an evaporating groundwater near an ancient surface below what is now the Sheepbed Member mudstone? Subsequent burial by the Sheepbed member and overlying strata might have led to the partial dissolution of this initial layer, which could be associated with the formation of the pure sulfate veins in Gale. Quantifying the depth of burial is problematic because, for instance, the Early Hesperian heat flow in Gale crater is unknown (see the Formation Model for the Gale crater Hydrous Ca-Sulfate Veins section). However, the early diagenetic, playa-related origin of the Watchet sulfate analogs, closely related to local changes in climate, surface water, and humidity (Talbot et al. 1994), suggests that they need not have been deeply buried (e.g., less than tens of meters) prior to formation of the gypsum veining, and that is our favored explanation for the MMG sulfates. We note, however, that up to 3.5 km of sediments were deposited in the Bristol Channel Basin (Philipp 2012) and that carbonate veins in the lower Jurassic (Blue Lias)—that overlies the MMG—may have originated at hundreds of meters of depth, so a deeper origin for the gypsum layers and veins now seen in the MMG cannot be ruled out in our study.

SUMMARY OF FORMATION CONDITIONS

Fluid Compositions

As was seen by the comparison of the Gale crater fluids with a variety of modeled, experimental, and selected terrestrial brines, the precipitation of clay minerals together with the lack of carbonates suggests that the Gale fluids were a CO_2-poor, neutral to alkaline groundwater-type fluid. Martian meteoric water could have contained some acid components (e.g., through volcanic exhalation or from impact interaction with the atmosphere, see Zolotov and Mironenko [2007] for an in-depth discussion). However, neutralization reactions of Martian basaltic rock compositions have been shown to be fast and efficient in experiments (Tosca and McLennan 2009) and models (Zolotov and Mironenko 2007). Carbonate precipitation would be expected from the presence of CO_2 (e.g., Fairén et al. 2004; Niles et al. 2009; Schwenzer et al. 2012a, 2012b; Melwani Daswani et al. 2016), but is not observed in the Yellowknife Bay mudstones by XRD (Vaniman et al. 2014), and SAM evolved gas analysis mass spectrometry indicates that, if carbonates are present at all, their abundance is below 1 wt% (Ming et al. 2014). Thus, the fluid at Yellowknife Bay, if originally in contact with acid and/or CO_2 sources from the atmosphere, would have been neutralized and lost their CO_2 content prior to the diagenetic reactions observed to form a Sheepbed Member type mudstone (Vaniman et al. 2014). This groundwater-type initial fluid (GPWox in our models, see the Model Conditions section and Bridges et al. 2015) reacted with pristine host rock, which contained magmatic minerals (olivine, pyroxene, plagioclase, sulfides) and potentially amorphous impact or volcanic glass. Bridges et al. (2015) assumed reactions to be incongruent, with a sequence of initial Mg leaching from olivine to form the cementations now visible as raised ridges, followed by the main alteration phase, which predominantly affected the amorphous phases and olivine (see Gíslason and Arnórsson 1993; Stefánsson et al. 2001; Hausrath and Brantley 2010; for discussion of the accompanying mineral formation and see Bridges et al. 2015; their section 4.5.1). Given the alteration phases observed, and more importantly the remaining olivine in the mudstones (Vaniman et al. 2014), the reaction likely did not progress beyond this stage, resulting in a dilute, neutral to alkaline fluid.

Fig. 10. Illustrated flow chart of potential processes leading to the precipitation of a "dirty sulfate layer" at Gale. The upper panel shows: A) precipitation of alteration minerals within the early sediments in a mixing zone between postimpact hydrothermal fluids and lake sediments heated by the underlying, fresh impact rocks; B) ascending fluids from the crater subsurface after cooling of the crater; C) periodical refilling of the lake from outside reservoirs; D) influx of smaller amounts of surface and near-surface waters through channels such as Peace Vallis. For details, see the Formation Model for the Gale crater Hydrous Ca-Sulfate Veins section. The lower panel shows the situation shortly after the deposition of a "dirty sulfate layer." Blue vein signatures indicate fractures transporting a groundwater-type fluid from underlying formations to shallower levels. Pink-blue areas indicate the shallow subsurface and potentially surface evaporation leading to a formation of the "dirty sulfate layer." The depth is dependent on uncertain factors such as the actual geothermal gradient in the area (see text, too).

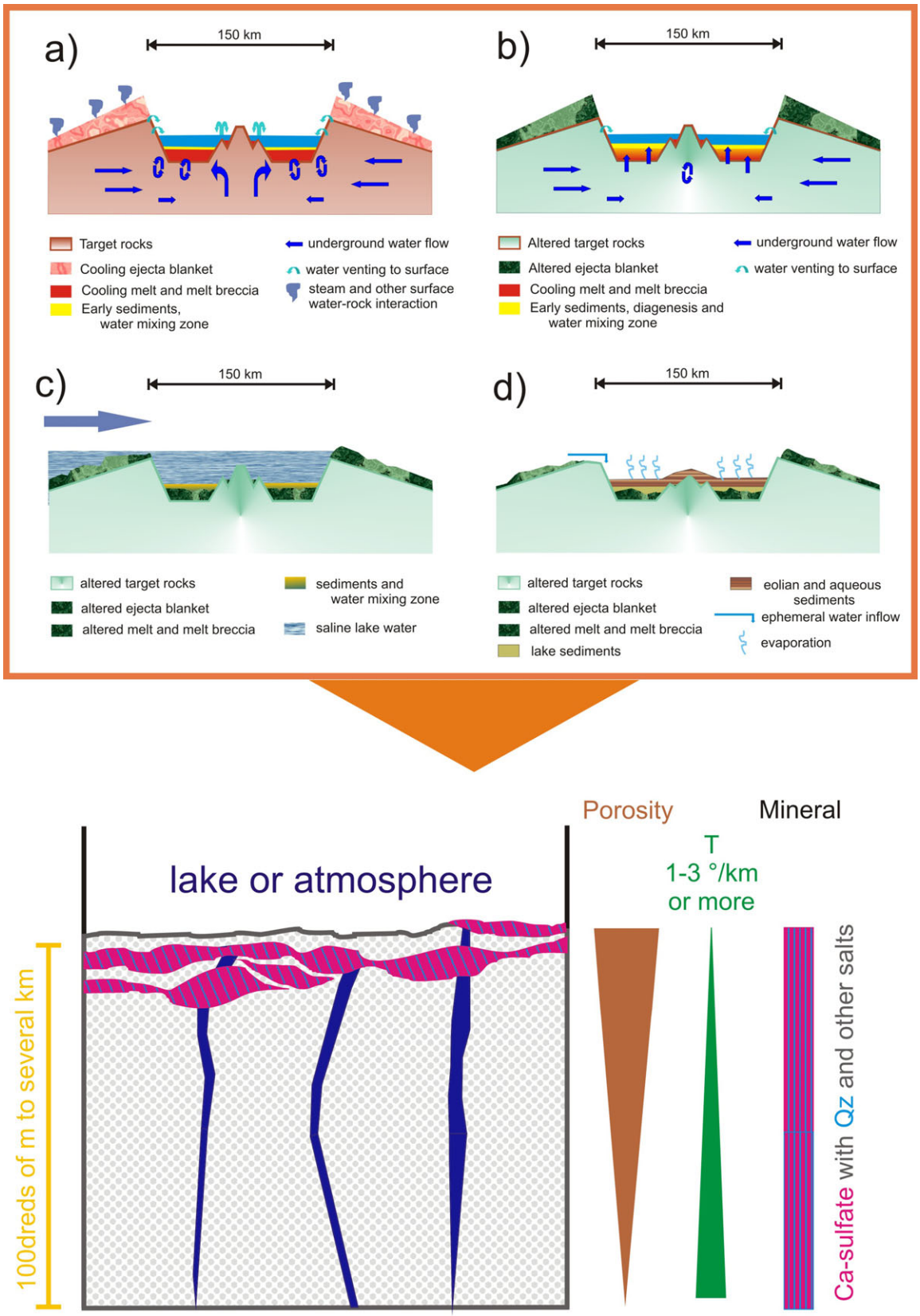
a)
150 km
Target rocks
Cooling ejecta blanket
Cooling melt and melt breccia
Early sediments, water mixing zone
underground water flow
water venting to surface
steam and other surface water-rock interaction
b)
150 km
Altered target rocks
Altered ejecta blanket
Cooling melt and melt breccia
Early sediments, diagenesis and water mixing zone
underground water flow
water venting to surface
c)
150 km
altered target rocks
altered ejecta blanket
altered melt and melt breccia
sediments and water mixing zone
saline lake water
d)
150 km
altered target rocks
altered ejecta blanket
altered melt and melt breccia
lake sediments
eolian and aqueous sediments
ephemeral water inflow
evaporation
lake or atmosphere
100dreds of m to several km
Porosity
Mineral
T
1-3 °/km
or more
Ca-sulfate with Qz and other salts

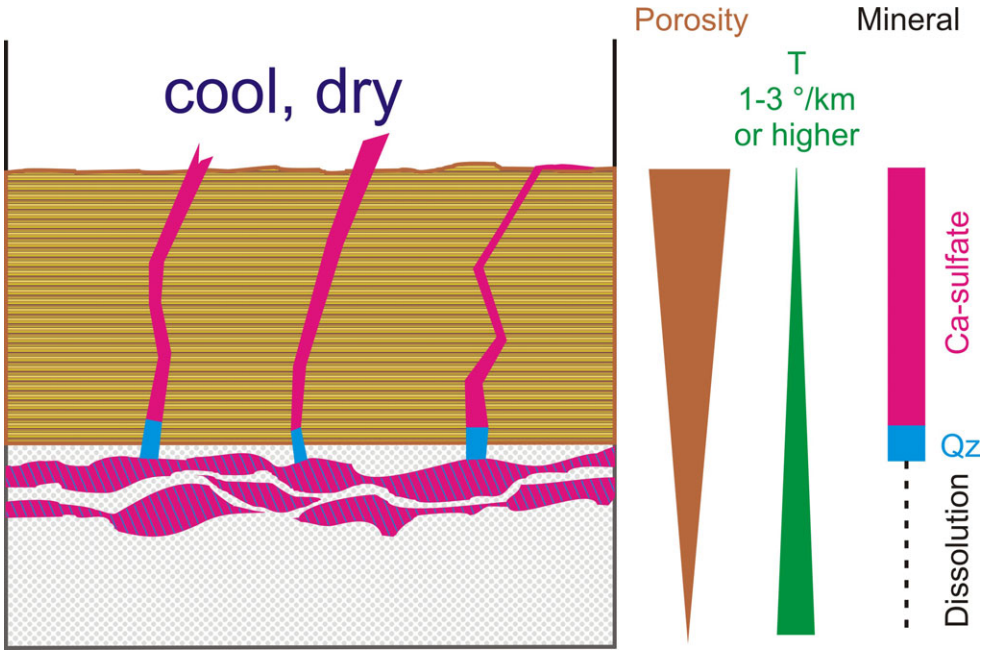

Fig. 11. Burial and re-mobilization of a "dirty sulfate layer." The original precipitate as formed by any or any combination of possibilities outlined in Fig. 10 could subsequently have been buried, exposing it to subsurface fluid dynamics, potentially warmer fluids than in the original depositional environment, higher pressure from the overlying sediments, and subsequent dissolution. The mobilization of the different components could have caused separation according to their solubility. Note that the formation with the dirty sulfate layer has not yet been found by Curiosity and could be much deeper than the rover's access, but the layer with the veins forming could be the Sheepbed or Murray formation with veins such as the Darwin outcrop or Garden City (Fig. 1). For details, see the Formation Model for the Gale crater Hydrous Ca-Sulfate Veins section.

Formation Model for the Gale crater Hydrous Ca-Sulfate Veins

This neutral to alkaline fluid would have formed the basis of the "groundwater" that could have been expelled from the pore space into fractures or filled Gale crater during its lake stages. As shown above, any precipitation directly from such a fluid, especially if cooling due to ascent along the geothermal gradient was involved, would have led to an assemblage of alteration minerals. For example, Catling (1999) describes an alteration sequence that involves silica and carbonates, which are not observed in the sulfate veins in Gale, and our models include silica as well as more soluble salts (e.g., Fig. 4).

Therefore, purification of the initial precipitate is required, which can generally be achieved through two processes: fractional crystallization or later refinement of an initial impure deposit. Fractionated crystallization would require a set of steps, including spatial separation of the fluid from the initial precipitates before the sulfate precipitation, and again before the precipitation of more soluble salts (Fig. 5), because the sulfate has a very pure composition.

We take this pure nature of the calcium sulfate as an indication that refinement of the initial deposit actually took place. In our two-step model, an initial mechanism precipitated S species, e.g., in a dirty sulfate layer. There could have been a time gap between the initial deposition, including accumulation of overlying sediments, and the next steps, which involve dissolution and re-precipitation as pure sulfates in the fractures. Possible first steps are (in chronological order, see also Fig. 10):

1. Impact-generated hydrothermal alteration: A crater the size of Gale has a deeply fractured underground, in which a large volume of rock beneath the crater could have been altered by hydrothermal systems active for an extended period of time (e.g., Abramov and Kring 2005; Schwenzer and Kring 2009, 2013). Hot fluids enhance alteration and thus leaching and could be responsible for the transport of a significant amount of salts from the underground into an initial postimpact crater lake. The upwelling fluid would necessarily have met a boundary with different conditions when venting either into an existing crater lake or subaerially. Such venting activity has been observed from orbit in the Martian Toro Crater (Fairén et al. 2010a, 2010b; Marzo et al. 2010). The

precipitation could thus be subaerial through evaporation or subaqueous through fluid mixing on the floor of this early crater lake, resulting in a "dirty sulfate layer," formed during the early history of Gale and buried by later sedimentation.

2. Postimpact diagenetic: If sedimentation of the first Gale lake sediments occurred within the window of activity of the hydrothermal system (several hundreds of thousands of years for a crater the size of Gale; Abramov and Kring 2005; Schwenzer et al. 2012a, 2012b), the still high postimpact geothermal gradient could have caused enhanced diagenesis of early sediments. This is observed in at least one terrestrial example, the 24 km diameter Boltysh Crater in the Ukraine (Watson et al. 2010; Williams et al. 2013a, 2013b). Warm fluids could have deposited a first, "dirty sulfate" enrichment within the earliest sediments, and become buried in the underground.
3. Sabkha-type environment precipitation: If, indeed, Mars was more water rich in its early history (e.g., Villanueva et al. 2015), Gale could have been connected with other reservoirs, especially groundwater transport from the highlands. Gale is the deepest location in this region of Mars, and all groundwater systems would have led to water seepage inside Gale crater. This could have led to a periodical refilling of Gale crater and subsequent evaporation, which could have caused sabkha-type precipitation (Essefi et al. 2014), and so produced layered and mixed, sulfate-bearing precipitates.
4. Ephemeral lake: Other transient sources of water could have included the inflow of precipitation or snow melt water through gaps in the crater rim, and/or from the highest reaches of Aeolis Mons (Fairén et al. 2014). Those could have fed a shallow, at times readily evaporating playa lake analogous to the Mercia Mudstone group analogies we described in the Evidence for Re-dissolution and Watchet Bay Terrestrial Analog: Geologic Similarities Between Gale crater, Mars, and the Mercia Mudstone Group, Watchet Bay, Upper Triassic, UK sections. The nature of the mudstone—conglomerate sequences observed at Gale (Grotzinger et al. 2014)—also supports this variation of the lake inflow regimes.

Our model assumes that all the precipitates and evaporites described under (1–4) would have been composed of a variety of salts and silica. Deduced from our analog study at Watchet Bay, burial of the dirty sulfate layer(s) would have occurred (Fig. 10). Subsequent redissolution of the initial deposit, likely due to upward migrating pore fluids during compaction, would have mobilized the more soluble salts and left other precipitates (e.g., SiO_2 polymorphs) behind (Fig. 11). This would have refined the secondary precipitate to form the pure sulfate observed in the Yellowknife Bay veins. Potentially, Curiosity has discovered geomorphological structures indicating subsurface void collapse that would accompany such a scenario (Wiens et al. 2015; Rubin et al. unpublished data). We, therefore, conclude that mobilization of a dirty sulfate layer, similar to what is observed in Triassic age sediments at Watchet Bay, UK, is the most likely process for the formation of pure Ca-sulfate in the Yellowknife Bay veins.

CONCLUSIONS

1. The diagenetic fluid in the Yellowknife mudstones was a dilute, slightly alkaline, CO_2-poor fluid with total dissolved solids ranging from 1.8×10^{-2} to 4.7×10^{-2} mole L^{-1} at T of 10 °C.
2. Mg depletion in the fluid relative to Deccan and other Mars fluids was a result of initial diagenetic smectite formation and associated early dissolution of olivine. Alkali elements (Na, K) stay in solution, which leads to a relative enrichment of (Na + K) over (Mg + Ca + Fe) compared with other Martian fluids (e.g., derived from alteration of the nakhlite meteorite composition) and terrestrial fluids (e.g., Deccan Traps).
3. Evaporation of this diagenetic fluid at Yellowknife Bay, Gale crater would have led to the formation of silica and sulfate-rich deposits.
4. Subsequent dissolution of such deposits—which we predict are present in the Gale sedimentary succession—led to the formation of pure sulfate veins seen in the Gale sediments along the Curiosity traverse.
5. The original precipitate likely was gypsum, which dehydrated after precipitation during burial and/or near-surface desiccation.
6. A terrestrial analog in the UK Triassic (Mercia Mudstone Group, Watchet Bay) supports the model of dissolution of a mixed silica and sulfate-rich shallow horizon to form pure sulfate veins.

Acknowledgments—We thank the two reviewers Brian Hynek and Sally Potter-McIntyre and AE Justin Filiberto for their insightful comments, which improved the presentation of this article. We are grateful to Mark H. Reed and his team for providing CHIM-XPT for this study. Support from the engineers, colleagues in operations roles, and staff of NASA Mars Science Laboratory Mission are gratefully acknowledged. JCB and SPS acknowledge funding from the UK Space Agency, SPS additional funding through an Open

University Research Investment Fellowship. F.W. acknowledges CNES funding.

Editorial Handling—Dr. Justin Filiberto

REFERENCES

Abramov O. and Kring D. A. 2005. Impact-induced hydrothermal activity on early Mars. *Journal of Geophysical Research* 110:E12S09. doi: 10.1029/2005JE002453.

Aiuppa A., Allard P., D'Alessandro W., Michel A., Parello F., Treuil M., and Valenza M. 2000. Mobility and fluxes of major, minor and trace metals during basalt weathering and groundwater transport at Mt. Etna volcano (Sicily). *Geochimica et Cosmochimica Acta* 64:1827–1841.

Anderson R., Bridges J. C., Williams A., Edgar L., Ollila A., Williams J., Nachon M., Mangold N., Fisk M., Schieber J., Gupta S., Dromart G., Wiens R., Le Mouélic S., Forni O., Lanza N., Mezzacappa A., Sautter V., Blaney D., Clark B., Clegg S., Gasnault O., Lasue J., Leveille R., Lewin E., Lewis K. W., Maurice S., Newson H., Schwenzer S. P., and Vaniman D. 2014. ChemCam results from the Shaler fluvial sedimentary outcrop in Gale Crater. *Icarus* 249:2–21. doi:10.1016/j.icarus.2014.07.025.

Arnórsson S., Gunnlaugsson E., and Svavarsson H. 1983. The chemistry of geothermal waters in Iceland. II. Mineral equilibria and independent variables controlling water compositions. *Geochimica et Cosmochimica Acta* 47:547–566.

Arnórsson S., Stefánsson A., and Bjarnason J. Ö. 2007. Fluid-fluid interactions in geothermal systems. *Reviews in Mineralogy & Geochemistry* 65:259–312.

Arvidson R. E., Squyres S. W., Bell J. F., Catalano J. G., Clark B. C., Crumpler L. S., De Souza P. A., Fairén A. G., Farrand W. H., Fox V. K., Gellert R., Ghosh A., Golombek M. P., Grotzinger J. P., Guinness E. A., Herkenhoff K. E., Jolliff B. L., Knoll A. H., Li R., Mclennan S. M., Ming D. W., Mittlefehldt D. W., Moore J. M., Morris R. V., Murchie S. L., Parker T. J., Paulsen G., Rice J. W., Ruff S. W., Smith M. D., and Wolff M. J. 2014. Ancient aqueous environments at Endeavour Crater, Mars. *Science* 343. doi:10.1126/science.1248097.

Baker L. L., Agenbroad D. J., and Wood S. A. 2000. Experimental hydrothermal alteration of a Martian analog basalt: Implications for Martian meteorites. *Meteoritics & Planetary Science* 35:31–38.

Bell J. F. III, McSween H. Y. Jr., Crisp J. A., Morris R. V., Murchie S. L., Bridges N. T., Johnson J. R., Britt D. T., Golombek M. P., Moore H. J., Ghosh A., Bishop J. L., Anderson R. C., Brückner J., Economou T., Greenwood J. P., Gunnlaugsson H. P., Hargraves R. M., Hviid S., Knudsen J. M., Madsen M. B., Reid R., Rieder R., and Soderblom L. 2000. Mineralogic and compositional properties of Martian soil and dust: Results from Mars Pathfinder. *Journal of Geophysical Research* 105:1721–1755.

Benedetti M. F., Dia A., Riotte J., Chabaux F., Gérard M., Boulégue J., Fritz B., Chauvel C., Bulourde M., Dérunelle B., and Ildefonse P. 2003. Chemical weathering of basaltic lava flows undergoing extreme climatic conditions: The water geochemistry record. *Chemical Geology* 201:1–17.

Bibring J.-P., Langevin Y., Gendrin A., Gondet B., Poulet F., Berthe M., Soufflot A., Arvidson R., Mangold N., Mustard J. F., and Drossart P. 2005. Mars surface diversity as revealed by the OMEGA/Mars express observations. *Science* 307:1576–1581.

Bibring J.-P., Langevin Y., Mustard J. F., Poulet F., Arvidson R., Gendrin A., Gondet B., Mangold N., Pinet P., Forget F., and the OMEGA team. 2006. Global mineralogical and aqueous Mars history derived from OMEGA/Mars Express Data. *Science* 312:400–404.

Brack A., Horneck G., Cockell C. S., Bérces A., Belisheva N. K., Eiroa C., Henning T., Herbst T., Kaltenegger L., Léger A., Liseau R., Lammer H., Selsis F., Beichman C., Danchi W., Fridlund M., Lunine J., Paresce F., Penny A., Quirrenbach A., Röttgering H., Schneider J., Stam D., Tinetti G., and White G. J. 2010. Origin and evolution of life on terrestrial planets. *Astrobiology* 10:69–76.

Bridges J. C. and Grady M. M. 2000. Evaporite minerals assemblages in the nakhlite (Martian) meteorites. *Earth and Planetary Science Letters* 176:267–279.

Bridges J. C. and Schwenzer S. P. 2012. The nakhlite hydrothermal brine on Mars. *Earth and Planetary Science Letters* 359–360:117–123.

Bridges J. C., Catling D. C., Saxton J. M., Swindle T. D., Lyon I. C., and Grady M. M. 2001. Alteration assemblages in Martian meteorites: Implications for near surface processes. *Space Science Reviews* 96:365–392.

Bridges J. C., Schwenzer S. P., Leveille R., Westall F., Wiens R., Mangold N., Bristow T., Edwards P., and Berger G. 2015. Diagenesis and clay formation at Gale Crater, Mars. *Journal of Geophysical Research* 120:1–19. doi:10.1002/2014JE004757.

Bullock M. A., Moore J. M., and Mellon M. T. 2004. Laboratory simulations of Mars aqueous geochemistry. *Icarus* 170:404–423.

Carbone M., Ballirano P., and Caminiti R. 2008. Kinetics of gypsum dehydration at reduced pressure: An energy dispersive X-ray diffraction study. *European Journal of Mineralogy* 20:621–627.

Carr M. 2006. *The surface of Mars*. Cambridge, UK: Cambridge: University Press. 307 p.

Carter J., Poulet F., Bibring J.-P., Mangold N., and Murchie S. 2013. Hydrous minerals on Mars as seen by the CRISM and OMEGA imaging spectrometers: Updated global view. *Journal of Geophysical Research* 118:831–858.

Catling D. C. 1999. A chemical model for evaporites on early Mars: Possible sedimentary tracers of the early climate and implications for exploration. *Journal of Geophysical Research* 104:16,453–16,469.

Changela H. G. and Bridges J. C. 2010. Alteration assemblages in the nakhlites: Variation with depth on Mars. *Meteoritics & Planetary Science* 45:1847–1867.

Clark B. C., Baird A. K., Rose H. J. Jr., , Toulmin P. III, Keil K., Castro A. J., Kelliher W. C., Rowe C. D., and Evans P. H. 1976. Inorganic analyses of Martian surface samples at the Viking Landing Sites. *Science* 194:1283–1288.

Cockell C. S., Balme M., Bridges J. C., Davila A., and Schwenzer S. P. 2012. Uninhabitated habitats on Mars. *Icarus* 217:184–193. doi:10.1016/j.icarus.2011.10.025.

Conrad P. G. 2014. Scratching the surface of Martian habitability. *Science* 346:1288–1289.

Das A. and Krishnaswami S. 2007. Elemental geochemistry of river sediments from Deccan Traps, India: Implications to sources of elements and their mobility during basalt–water interaction. *Chemical Geology* 242:232–254.

Das A., Krishnaswami S., Sarin M. M., and Pande K. 2005. Chemical weathering in the Krishna Basin and Western Ghats of the Deccan Traps, Idia: Rates of basalt weathering and their controls. *Geochimica et Cosmochimica Acta* 69:2067–2084.

DeBraal J. D., Reed M. H., and Plumlee G. S. 1993. Calculated mineral precipitation upon evaporation of a model Martian groundwater near 0 °C. Workshop on Chemical Weathering on Mars. LPI Technical Report 92-04, 10–11.

Dickinson W. W. and Rosen M. R. 2014. Antarctic permafrost: An analogue for water and diagenetic minerals on Mars. *Geology* 31:199–202.

Drever J. I. 1988. *The Geochemistry of natural waters*, 2nd ed. Upper Saddle River, New Jersey: Prentice Hall. 437 pp.

Eckhardt F. D., Bryant R. G., McCulloch G., Spiro B., and Wood W. W. 2008. The hydrochemistry of a semi-arid pan basin case study: Sua Pan, Makgadikgadi, Botswana. *Applied Geochemistry* 23:1563–1580.

Elsenousy A., Hanley J., and Chevrier V. 2015. Effect of evaporation and freezing on the salt paragenesis and habitability of brines at the Phoenix landing site. *Earth and Planetary Science Letters* 421:39–46.

Essefi E., Komatsu G., Fairén A. G., Chan M. A., and Yaich C. 2014. Groundwater influence on the aeolian sequence stratigraphy of the Mechertate-Chrita-Sidi El Hani system, Tunisian Sahel: Analogies to the wet-dry aeolian sequence stratigraphy at Meridiani Planum, Terby Crater, and Gale Crater, Mars. *Planetary and Space Science* 95:56–78.

Eugster H. P. 1986. Minerals in hot water. *American Mineralogist* 71:655–673.

Fairén A. G., Fernández-Remolar D., Dohm J. M., Baker V. R., and Amils R. 2004. Inhibition of carbonate synthesis in acidic oceans on early Mars. *Nature* 431:423–426.

Fairén A. G., Davila A. F., Duport L. G., Amils R., and Mckay C. 2009. Stability against freezing of aqueous solutions on early Mars. *Nature* 459:401–404.

Fairén A. G., Davila A. F., Lim D., Bramall N., Bonaccorsi R., Zavaleta J., Uceda E. R., Stoker C., Wierzchos J., Amils R., Dohm J. M., Andersen D., and McKay C. 2010a. Astrobiology through the ages of Mars. *Astrobiology* 10:821–843.

Fairén A. G., Chevrier V., Abramov O. Marzo G. A., Gavin P., Davila A. F., Bishop J. L., Roush T. L., Gross C., Kneissl T., Uceda E. R., Dohm J. M., Schulze-Makuch D., Rodríguez J. A. P., Amils R., and McKay C. P. 2010b. Noachian and more recent phyllosilicates in impact craters on Mars. *Proceedings of the National Academy of Sciences* 107:12,095–12,100.

Fairén A. G., Stokes C., Davies N., Schulze-Makuch D., Rodríguez J. A. P., Davila A. F., Uceda E. R., Dohm J. M., Baker V. R., Clifford S. M., McKay C. P., and Squyres S. W. 2014. A cold hydrological system in Gale crater, Mars. *Planetary & Space Science* 93–94:101–118.

Filiberto J. and Schwenzer S. P. 2013. Alteration mineralogy of the Home Plate and Columbia Hills—Formation conditions in context to impact, volcanism and fluvial activity. *Meteoritics & Planetary Science* 48:1937–1957. doi:10.1111/maps.12207.

Gaillard F., Michalski J., Berger G., McLennan S. M., and Scalliet B. 2013. Geochemical reservoirs and timing of sulfur cycling on Mars. *Space Science Reviews* 174:251–300.

Gellert R., Rieder R., Brückner J., Clark B. C., Dreibus G., Klingelhöfer G., Lugmair G. W., Ming D. W., Wänke H., Yen A., Zipfel J., and Squyres S. W. 2006. Alpha particle X-ray spectrometer (APXS): Results from Gusev Crater and calibration report. *Journal of Geophysical Research*, 111:E02S05. doi:10.1029/2005JE002555.

Gellert R., Berger J. A., Boyd N., Brunet C., Campbell J. L., Curry M., Elliott B., Fulford P., Grotzinger J., Hipkin V., Hurowitz J. A., King P. L., Leshin L. A., Limonadi D., Pavri B., Marchand G., Perrett G. M., Scodary A., Simmonds J. J., Spray J., Squyres S. W., Thompson L., VanBommel S., Pradler I., Yen A. S., and the MSL Science Team. 2013. Initial MSL APXS activities and observations at Gale Crater, Mars (abstract #1432). 44th Lunar and Planetary Science Conference. CD-ROM.

Gendrin A., Mangold N., Bibring J.-P., Langevin Y., Gondet B., Poulet F., Bonello G., Quantin C., Mustard J., Arvidson R., and LeMouélic S. 2005. Sulfates in Martian layered terrains: The OMEGA/Mars Express view. *Science* 307:1587–1591.

Gíslason S. R. and Arnórsson S. 1993. Dissolution of primary basaltic minerals in natural waters: Saturation state and kinetics. *Chemical Geology* 105:117–135.

Glavin D. P., Freissinet C., Miller K. E., Eigenbrode J. L., Brunner A. E., Buch A., Sutter B., Archer Jr. P. D., Atreya S. K., Brinckerhoff W. B., Cabane M., Coll P., Conrad P. G., Coscia D., Dworkin J. P., Franz H. B., Grotzinger J. P., Leshin L. A., Martin M. G., McKay C., Ming D. W., Navarro-González R., Pavlov A., Steele A., Summons R. E., Szopa C., Teinturier S. and Mahaffy P. R. 2013. Evidence for perchlorates and the origin of chlorinated hydrocarbons detected by SAM at the Rocknest aeolian deposit. *Journal of Geophysical Research: Planets* 118:1955–1973. doi:10.1002/jgre.20144.

Grotzinger J. P., Arvidson R. E., Bell J. F. III, Calvin W., Clark B. C., Fike D. A., Golombek M., Greeley R., Haldemann A., Herkenhoff K. E., Jolliff B. L., Knoll A. H., Malin M., McLennan S. M., Parker T., Soderblom L., Sohl-Dickstein S. N., Squyres S. W., Tosca N. J., and Watters W. A. 2005. Stratigraphy and sedimentology of a dry to wet eolian depositional system, Burns Formation, Meridiani Planum, Mars. *Earth and Planetary Science Letters* 240:11–72.

Grotzinger J. P., Sumner D. Y., Kah L. C., Stack K., Gupta S., Edgar L., Rubin D., Lewis K., Schieber J., Mangold N., Milliken R., Conrad P. G., DesMarais D., Farmer J., Siebach K., Calef F. III, Hurowitz J., McLennan S. M., Ming D., Vaniman D., Crisp J., Vasavada A., Edgett K. S., Malin M., Blake D., Gellert R., Mahaffy P., Wiens R. C., Maurice S., Grant J. A., Wilson S., Anderson R. C., Beegle L., Arvidson R., Hallet B., Sletten R. S., Rice M., Bell J. III, Griffes J., Ehlmann B., Anderson R. B., Bristow T. F., Dietrich W. E., Dromart G., Eigenbrode J., Fraeman A., Hardgrove C., Herkenhoff K., Jandura L., Kocurek G., Lee S., Leshin L. A., Leveille R., Limonadi D., Maki J., McCloskey S., Meyer M., Minitti M., Newsom H., Oehler D., Okon A., Palucis M., Parker T., Rowland S., Schmidt M., Squyres S., Steele A., Stolper E., Summons R., Treiman A., Williams R., Yingst A., and the MSL Science Team. 2014. A habitable fluvio-lacustrine environment at Yellowknife Bay, Gale Crater, Mars. *Science* 343. doi:10.1126/science.1242777.

Gudbrandsson S., Wolff-Boenisch D., Gislason S. R., and Oelkers E. H. 2011. An experimental study of crystalline basalt dissolution from $2 \leq$ pH ≤ 11 and temperatures

from 5 to 75 °C. *Geochimica et Cosmochimica Acta* 75:5496–5509.

Hallis L. J. and Taylor G. J. 2011. Comparisons of the four Miller Range nakhlites, MIL 03346, 090030, 090032 and 090136: Textural and compositional observations of primary and secondary mineral assemblages. *Meteoritics & Planetary Science* 46:1787–1803.

Hardie L. A. and Eugster H. P. 1970. The evolution of closed-basin brines. *Mineralogical Society of America Special Paper* 3:273–290.

Harvey R. P. and McSween H. Y. Jr. 1996. A possible high-temperature origin for the carbonates in the Martian meteorite ALH 84001. *Nature* 382:49–51.

Hausrath E. M. and Brantley S. L. 2010. Basalt and olivine dissolution under cold, salty and acidic conditions: What can we learn about recent aqueous weathering on Mars? *Journal of Geophysical Research* 115:E12001. doi:10.1029/2010JE003610.

Hicks L. J., Bridges J. C., and Gurman S. J. 2014. Ferric saponite and serpentine in the nakhlite Martian meteorites. *Geochimica et Cosmochimica Acta* 136:194–210.

Hounslow M. W., Posaen P. E., and Warrington G. 2004. Magnetostratigraphy and biostratigraphy of the Upper Triassic and lowermost Jurassic succession, St. Audrie's Bay, UK. *Palaeogeography, Palaeoclimatology, Palaeoecology* 213:331–358.

Howard A. S., Warrington G., Ambrose K., and Rees J. G. 2008. A formational framework for the Mercia Mudstone Group (Triassic) of England and Wales. British Geological Survey, Research report RR/08/04. 41 p.

Hudec P. P. and Sonnenfield P. 1980. Comparison of Caribbean solar ponds with inland solar lakes of British Columbia. In *Developments in sedimentology*, vol. 28, edited by Nissenbaum A. Hypersaline Brines and Evaporitic Environments. Amsterdam: Elsevier. 270 p.

Hurowitz J. A., McLennan S. M., Lindsley D. H., and Schoonen M. A. A. 2005. Experimental epithermal alteration of synthetic Los Angeles meteorite: Implications for the origin of Martian soils and identification of hydrothermal sites on Mars. *Journal of Geophysical Research* 110:22 p. doi:10.1029/2004JE002391.

Hurowitz J. A., McLennan S. M., Tosca N. J., Arvidson R. E., Michalski J. R., Ming D. W., Schröder C., and Squyres W. 2006. In situ and experimmental evidence for acidic weathering of rocks and soils on Mars. *Jourrnal of Geophysical Research* 111:E02S19. doi:10.1029/2005JE002515.

Jones B. F., Eugster H. P., and Rettig S. L. 1977. Hydrochemistry of the Lake Magadi Basin, Kenya. *Geochimica et Cosmochimica Acta* 41:53–72.

Kempe S. and Degens E. T. 1985. An early soda ocean? *Chemical Geology* 53:95–108.

King P. L., Lescinsky D. T., and Nesbitt H. W. 2004. The composition and evolution of primordial solutions on Mars, with application to other planetary bodies. *Geochimica et Cosmochimica Acta* 68:4993–5008.

Kounaves S. P., Hecht M. H., Kapit J., Quinn R. C., Catling D. C., Clark B. C., Ming D. W., Gospodinova K., Hredzak P., McElhoney K., and Shusterman J. 2010. Soluble sulfate in the Martian soil at the Phoenix landing site. *Geophysical Research Letters* 37:5 p. doi:10.1029/2010GL042613.

Kronyak R. E., Kah L. C., Nachon M., Mangold N., Wiens R. C., Williams R., Schieber J., and Grotzinger J. 2015. Distribution of mineralized veinsfrom Yellowknife Bay to Mount Sharp, Gale Crater, Mars: Insight from textural and compositional variation (abstract #1903). 46th Lunar and Planetary Science Conference. CD-ROM.

Langevin Y., Poulet F., Bibring J. P., and Gondet B. 2005. Sulfates in the North Polar Region of Mars detected by OMEGA/Mars Express. *Science* 307:1584–1586.

Last W. M. 1989. Continental brines and evaporites of the northern Great Plains of Canada. *Sedimentary Geology* 64:207–221.

Leshin L. A., et al. 2013. Volatile, isotope, and organic analysis of Martian fines with the Mars Curiosity rover. *Science* 341. doi:10.1126/science.1238937.

Léveillé R. J., Bridges J., Wiens R. C., Mangold N., Cousin A., Lanza N., Forni O., Ollila A., Grotzinger J., Clegg S., Siebach K., Berger G., Clarck B., Fabre C., Anderson R., Gasnault O., Blaney D., Deflores L., Leshin L., Sylvestre M., and Newsom H. 2014. Chemistry of fracture-filling raised ridges in Yellowknife Bay, Gale Crater: Window into past aqueous activity and habitability on Mars. *Journal of Geophysical Research* 119:2398–2415. doi:10.1002/2014JE004620.

Loges A., Wagner T., Kirnbauer T., Göb S., Bau M., Berner Z., and Markl G. 2012. Source and origin of active and fossil thermal spring systems, northern Upper Rhine Graben, Germany. *Applied Geochemistry* 27:1153–1169.

Marion G. M., Kargel J. S., and Catling D. C. 2008. Modeling ferrous–ferric iron chemistry with application to Martian surface geochemistry. *Geochimica et Cosmochimica Acta* 72:242–266.

Marucci E. C. and Hynek B. M. 2014. Laboratory simulations of acid-sulfate weathering under volcanic hydrothermal conditions: Implications for early Mars. *Journal of Geophysical Research* 119:679–703.

Marzo G. A., Davila A. F., Tornabene L. L., Dohm J. M., Fairen A. G., Gross C., Kneissl T., Bishop J. L., Roush T. L., and McKay C. P. 2010. Evidence for hesperian impact-induced hydrothermalism on Mars. *Icarus* 208:667–683.

McAdam A. C., Zolotov M. Y., Mironenko M. V., and Sharp G. 2008. Formation of silica by low temperature acid alteration of Martian rocks: Physical-chemical constraints. *Journal of Geophysical Research* 113:8 p. doi: 10.1029/2007JE003056.

McLennan S. M., Bell J. F. II, Calvin W. M., Christensen P. R., Clark B. C., de Souza P. A., Farmer J., Farrand W. H., Fike D. A., Gellert R., Shosh A., Glotch T. D., Grotzinger J. P., Han B., Herkenhoff K. E., Hurowitz J. A., Johnson J. R., Johnson S. S., Joliff B., Klingelhöfer G., Knoll A. H., Learner Z., Malino M. C., McSween H. Y., Pocock J., Ruff S. W., Sonderblom L. A., Squyres S. W., Tosca N. J., Watters W. A., Wyatt M. B., and Yen A. 2005. Provenance and diagenesis of the evaporite-bearing Burns formation, Meridiani Planum, Mars. *Earth and Planetary Science Letters* 240:95–121.

McLennan S. M., Anderson R. B., Bell J. F. III, Bridges J. C., Calef F. III, Campbell J. L., Clark B. C., Clegg S., Conrad P., Cousin A., Des Marais D. J., Dromart G., Dyar M. D., Edgar L. A., Ehlmann B. L., Fabre C., Forni O., Gasnault O., Gellert R., Gordon S., Grant J. A., Grotzinger J. P., Gupta S., Herkenhoff K. E., Hurowitz J. A., King P. L., Le Mouélic S., Leshin L. A., Léveillé R., Lewis K. W., Mangold N., Maurice D. W., Ming R. V., Morris M., Nachon H. E., Newsom A. M., Ollila G. M., Perrett M. S.,

Rice M. E., Schmidt S. P., Schwenzer K., Stack E. M., Stolper D. Y., Sumner A. H., Treiman S., VanBommel D. T., Vaniman A., Vasavada R. C., and Wiens R. A. Yingst 2014. Elemental geochemistry of sedimentary rocks in Yellowknife Bay, Gale Crater, Mars. *Science* 343. doi:10.1126/science.1244734.

Melwani Daswani M., Schwenzer S. P., Reed M. H., Wright I. P., and Grady M. G. 2016. Alteration minerals, fluids and gases on early Mars: Predictions from 1D flow geochemical modelling of mineral assemblages in meteorite ALH 84001. *Meteoritics & Planetary Science*, doi: 10.1111/maps.12713.

Ming D. W., Archer P. D. Jr., Glavin D. P., Eigenbrode J. L., Franz H. B., Sutter B., Brunner A. E., Stern J. C., Freissinet C., McAdam A. C., Mahaffy P. R., Cabane M., Coll P., Campbell J. L., Atreya S. K., Niles P. B., Bell J. F. III, Bish D. L., Brinckerhoff W. B., Buch A., Conrad P. G., Des Marais D. J., Ehlmann B. L., Fairén A. G., Farley K., Flesch G. J., Francois P., Gellert R., Grant J. A., Grotzinger J. P., Gupta S., Herkenhoff K. E., Hurowitz J. A., Leshin L. A., Lewis K. W., McLennan S. M., Miller K. E., Moersch J., Morris R. V., Navarro-González R., Pavlov A. A., Perrett G. M., Pradler I., Squyres S. W., Summons R. E., Steele A., Stolper E. M., Sumner D. Y., Szopa C., Teinturier S., Trainer M. G., Treiman A. H., Vaniman D. T., Vasavada A. R., Webster C. R., Wray J. J., Yingst R. A., and the MSL Science Team. 2014. Volatile and organic compositions of sedimentary rocks in Yellowknife Bay, Gale crater, Mars. *Science* 343. doi:10.1126/science.1245267.

Minissale A., Vaselli O., Chandrasekharam D., Magro G., Tassi F., and Casiglia A. 2000. Origin and evolution of "intracratonic" thermal fluids from central-western peninsular India. *Earth and Planetary Science Letters* 181:377–394.

Moore J. M. and Bullock M. A. 1999. Experimental studies of Mars-analog brines. *Journal of Geophysical Research* 104:21,925–21,934.

Moore J. M., Bullock M. A., Newsom H., and Nelson M. 2010. Laboratory simulations of Mars evaporite geochemistry. *Journal of Geophysical Research* 115:11 p. doi:10.1029/2008JE003208.

Morris R. V., Ming D. W., Blake D. F., Vaniman D. T., Bish D. L., Chipera S. J., Downs R. T., Gellert R., Treiman A. H., Yen A. S., Achilles C. N., Anderson R. C., Bristow T. F., Crisp J. A., Des Marais D. J., Farmer J. D., Grotzinger J. P., Leshin L. A., McAdam A. C., Morookian J. M., Morrison S. M., Rampe E. B., Sarrazin P. C., Spanovich N., Stolper E. M., and the MSL Science Team. 2013. The amorphous component in Martian basaltic soil in global perspective from MSL and MER Missions (abstract #1653). 44th Lunar and Planetary Science Conference. CD-ROM.

Morris R.V, Ming D. W., Gellert R., Vaniman D. T., Bish D. L., Blake D. F., Chipera S. J., Downs R. T., Treiman A. H., Yen A. S., Achilles C. N., Archer P. D., Bristow T. F., Crisp J. A., Des Marais D. J., Farmer J. D., Grotzinger J. P., Mahaffy P. R., McAdam A. C., Morookian J. M., Morrison S. M., Rampe E. B., and the MSL Science Team. 2014. Chemical composition of crystalline, smectite, and amorphous components for Rocknest soil and John Klein and Cumberland mudstone drill fines using APXS, CheMin, and SAM data sets from Gale Crater, Mars (abstract #1319). 45th Lunar and Planetary Science Conference. CD-ROM.

Mustard J. F., Murchie S., Pelkey S. M., Ehlmann B. L., Milliken R. E., Grant J. A., Bibring J. P., Poulet F., Bishop J., Noe Dobrea E. Z., Roach L., Seelos F., Arvidson R., Wiseman S., Green R., Hash C., Humm D., Malaret E., McGovern J. A., Seelos K., Clancy T., Clark R., Des Marais D., Izenberg N., Knudson A., Langevin Y., Martin T., McGuire P., Morris R., Robinson M., Roush T., Smith M., Swayze G., Taylor H., Titus T., and Wolff M. 2008. Hydrated silicate minerals on Mars observed by the Mars Reconnaissance Orbiter CRISM instrument. *Nature* 454:305–309.

Nachon M., Clegg S. M., Mangold N., Schröder S., Kah L. C., Dromart G., Ollila A., Johnson J. R., Oehler D. Z., Bridges J. C., Le Mouélic S., Forni O., Wiens R. C., Anderson R. B., Blaney D. L., Bell J. F. III, Clark B., Cousin A., Dyar M. D., Ehlmann B., Fabre C., Gasnault O., Grotzinger J., Lasue J., Lewin E., Léveillé R., McLennan S., Maurice S., Meslin P.-Y., Rapin W., Rice M., Squyres S. W., Stack K., Sumner D. Y., Vaniman D., and Wellington D. 2014. Calcium sulfate veins characterized by ChemCam/Curiosity at Gale Crater, Mars. *Journal of Geophysical Research* 119:1991–2016. doi: 10.1002/2013JE004588.

Niles P. B., Zolotov M. Y., and Leshin L. A. 2009. Insights into the formation of Fe- and Mg-rich aqueous solutions on early Mars provided by the ALH 84001 carbonates. *Earth and Planetary Science Letters* 286:122–130.

Ossorio M., van Driessche A. E. S., Pérez P., and García-Ruiz J. M. 2014. The gypsum–anhydrite paradox revisited. *Chemical Geology* 386:16–21.

Peacock D. C. P. and Sanderson D. J. 1999. Deformation history and basin-controlling faults in the Mesozoic sedimentary rocks of the Somerset coast. *Proceedings of the Geologists' Association* 110:41–52.

Philipp S. L. 2008. Geometry and formation of gypsum veins in mudstones at Watchet, Somerset, SW England. *Geological Magazine* 145:831–844.

Philipp S. L. 2012. Fluid overpressure estimates from the aspect ratios of mineral veins. *Tectonophysics* 581:35–47.

Rapin W., Meslin P.-Y., Schröder S., Nachon M., Cousin A., Maurcie S., Wiens R. C., Lasue J., Blank J., and Belgacem I. 2015. Hydration state of calcium sulfate veins as observed by the ChemCam instrument (abstract #2966). 46th Lunar and Planetary Science Conference. CD-ROM.

Reed M. H. 1982. Calculation of multicomponent chemical equilibria and reaction processes in systems involving minerals, gases and an aqueous phase. *Geochimica et Cosmochimica Acta* 46:513–528.

Reed M. H. 1983. Seawater-basalt reaction and the origin of greenstones and related ore deposits. *Economic Geology* 78:466–485.

Reed M. H. and Spycher N. F. 2006. *User guide for CHILLER: A program for computing water-rock reactions, boiling, mixing, and other reaction processes in aqueous-mineral-gas systems and Minplot guide*, 3rd edn. Eugene, Oregon: University of Oregon.

Reed M. H., Spycher N. F., and Palandri J. 2010. *User guide for CHIM-XPT: A program for computing reaction processes in aqueous-mineral-gas systems and Minplot guide*. Eugene, Oregon: University of Oregon.

Rieder R., Gellert R., Anderson R. C., Brückner J., Clark B. C., Dreibus G., Economou T., Klingelhöfer G., Lugmair G. W., Ming D. W., Squyres S. W., d'Uston C., Wänke H., Yen A., and Zipfel J. 2004. Chemisty of rocks and

soils at Meridiani Planum from the alpha particle X-ray spectrometer. *Science* 306:1746–1749.

Robertson K. and Bish D. 2013. Constraints on the distribution of $CaSO_4*nH_2O$ phases on Mars and implications for their contribution to the hydrological cycle. *Icarus* 223:407–417.

Sawyer D. J., McGehee M. D., Canepa J., and Moore C. B. 2000. Water soluble ions in the Nakhla Martian meteorite. *Meteoritics & Planetary Science* 35:143–141.

Schieber J., Gupta S., Grotzinger J., and Suarez-Rivera R. and the MSL Science Team. 2013. Hydraulic fracturing of Martian mudstones (abstract # 9). Geological Society of America meeting, Denver, Colorado, 27–30, October 2013.

Schmidt M. E., Campbell J. L., Gellert R., Perrett G. M., Treiman A. H., Blaney D. L., Olilla A., Calef F. J. III, Edgar L., Elliott B. E., Grotzinger J., Hurowitz J., King P. L., Minitti M. E., Sautter V., Stack K., Berger J. A., Bridges J. C., Ehlmann B. L., Forni O., Leshin L. A., Lewis K. W., McLennan S. M., Ming D. W., Newsom H., Pradler I., Squyres S. W., Stolper E. M., Thompson L., van Bommel S., Wiens R. C., and the MSL Science Team. 2014. Geochemical diversity in first rocks examined by the Curiosity Rover in Gale Crater: Evidence for and significance of an alkali and volatile-rich igneous source. *Journal of Geophysical Research* 119:64–81.

Schreiber B. C. and el Tabakh M. 2000. Deposition and early alteration of evaporites. *Sedimentology* 47:215–238.

Schroeder S., Meslin P.-Y., Gasnault O., Maurice S., Cousin A., Forni O., Manglod N., Rapin W., Le Mouelic S., Ollila A., Nachon M., Lasue J., Dyar M. D., Clegg S., Jackson R., and Wiens R. C. 2015. First analysis of the hydrogen signal in ChemCham LIBS spectra. *Icarus* 249:43–61.

Schwenzer S. P. and Kring D. A. 2009. Impact-generated hydrothermal systems: Capable of forming phyllosilicates on Noachian Mars. *Geology* 37:1091–1094.

Schwenzer S. P. and Kring D. A. 2013. Alteration minerals in impact-generated hydrothermal systems—Exploring host rock variability. *Icarus* 226:487–496.

Schwenzer S. P., Abramov O., Allen C. C., Bridges J. C., Clifford S. M., Filiberto J., Kring D. A., Lasue J., McGovern P. J., Newsom H. E., Treiman A. H., Vaniman D. T., Wiens R. C., and Wittmann A. 2012a. Gale Crater: Formation and post-impact hydrous environments. *Planetary and Space Science* 70:84–95.

Schwenzer S. P., Abramov O., Allen C. C., Clifford S. M., Cockell C. S., Filiberto J., Kring D. A., Lasue J., McGovern P. J., Newsom H. E., Treiman A. H., Vaniman D. T., and Wiens R. C. 2012b. Puncturing Mars: How impact craters interact with the Martian cryosphere. *Earth and Planetary Science Letters* 335–336:9–17.

Schwenzer S. P., Bridges J., Leveille R. J., Westall F., Wiens R. C., Mangold N., McAdam A., Conrad P. G., Martín-Torres J., and Zorzano M. P. 2014. Fluids and sulfate vein formation in Gale Crater, Mars. AGU Fall meeting 2014, abstract #P42C-08.

Schwenzer S. P., Bullock M. A., Bridges J. C., Chavez C. L., Filiberto J., Hicks L. J., Kelley S. P., Miller M. A., Moore J. M., Smith H. D., Swindle T. D., and Treiman A. H. 2016a. Noble gas fractionation in hydrous rock alteration under diagenetic pressure and temperature conditions (abstract #1889). 47th Lunar and Planetary Science Conference. CD-ROM.

Schwenzer S. P., Bridges J. C., McAdam A., Steer E. D., Conrad P. G., Kelley S. P., and Wiens R. C. 2016b. Modelling sulfide microenvironments on Mars (abstract #1886). 47th Lunar and Planetary Science Conference. CD-ROM.

Siebach K. L., Grotzinger J. P., Kah L. C., Stack K. M., Malin M., Léveillé R., and Sumner D. Y. 2014. Subaqueous shrinkage cracks in the Sheepbed Mudstone: Implications for early fluid diagenesis, Gale Crater, Mars. *Journal of Geophysical Research* 119:1597–1613. doi: 10.1002/2014JE004623.

Smedley P. L. 2010. A survey of the inorganic chemistry of bottle mineral waters from the British Isles. *Applied Geochemistry* 25:1872–1888.

Smith P. H., Tamppari L. K., Arvidson R. E., Bass D., Blaney D., Boyton W. V., Carswell A., Catling D. C., Clark B. C., Duck T., DeJong E., Fisher D., Goetz W., Gunnlaugsson H. P., Hecht M. H., Hipking V., Hoffman J., Hviid S. F., Keller H. U., Kounaves S. P., Lange C. F., Lemmon M. T., Madsen M. B., Markiewicz W. J., Marshall J., McKay C. P., Mellon M. T., Ming D. W., Morris R. V., Pike W. T., Renno N., Staufer U., Stoker C., Taylor P., Whiteway J. A., and Zent A. P. 2009. H_2O at the Phoenix landing site. *Science* 325:58–61.

Squyres S. W., Arvidson R. E., Bell J. F. III, Brückner J., Cabrol N. A., Calvin W., Carr M. H., Christensen P. R., Clark B. C., Crumpler L., Des Marais D. J., d'Uston C., Economou T., Farmer J., Farrand W., Folkner W., Golombek M., Gorevan S., Grant J. A., Greeley R., Grotzinger J., Haskin L., Herkenhoff K. E., Hviid S., Johnson J., Klingelhöfer G., Knoll A. H., Landis G., Lemmon M., Li R., Madsen M. B., Malin M. C., McLennan S. M., McSween H. Y., Ming D. W., Moersch J., Morris J., Parker T., Rice J. W. Jr., Richter L., Rieder R., Sims M., Smith M., Smith P., Sonderblom L. A., Sullivan R., Wänke H., Wdowiak T., Wolff M., and Yen A. 2004. The Opportunity Rover's Athena science investigation at Meridiani Planum, Mars. *Science* 306:1698–1703.

Squyres S. W., Arvidson R. E., Ruff S., Gellert R., Morris R. V., Ming D. W., Crumpler L., Farmer J. D., Des Marais D. J., Yen A., McLennan S. M., Calvin W., Bell J. F. III, Clark B. C., Wang A., McCoy T. J., Schmidt M. E., and de Souza P. A. Jr. 2008. Detection of silica-rich deposits on Mars. *Science* 320:1063–1067.

Squyres S. W., Arvidson R. E., Bell J. F. III, Calef F. III, Clark B. C., Cohen B. A., Crumpler L. A., de Souza P. A. Jr., Farrand W. H., Gellert R., Grant J., Herkenhoff K. E., Hurowitz J. A., Johnson J. R., Jolliff B. L., Knoll A. H., Li R., McLennan S. M., Ming D. W., Mittlehfehldt D. W., Parker T. J., Paulsen G., Rice M. S., Ruff S. W., Schröder C., Yen A. S., and Zacny K. 2012. Ancient impact and aqueous processes at endeavour crater, Mars. *Science* 336:570–576.

Stack K. M., Grotzinger J. P., Kah L. C., Schmidt M. E., Mangold N., Edgett K. S., Sumner D. Y., Siebach K. L., Nachon M., Lee R., Blaney D. L., Deflores L. P., Edgar L. A., Fairén A. G., Leshin L. A., Maurice S., Oehler D. Z., Rice M. S., and Wiens R. C. 2015. Diagenetic origin of nodules in the Sheepbed member, Yellowknife Bay formation, Gale crater, Mars. *Journal of Geophysical Research* 119:1637–1664. doi:10.1002/2014JE004617.

Stefánsson A., Gíslason S. R., and Arnórsson S. 2001. Dissolution of primary minerals in natural waters II: Mineral saturation state. *Chemical Geology* 172:251–276.

Stern J. C., Sutter B., McKay C. P., Navarro-González R., Freissinet C., Conrad P. G., Mahaffy P. R., Archer P. D. Jr., Ming D. W., Niles P. B., Zorzano M.-P., Martin-Torres F. J., and the MSL Science Team. 2015. The nitrate/perchlorate ratio on Mars as an indicator for habitability (abstract #2590). 46th Lunar and Planetary Science Conference. CD-ROM.

Stolper E. M., Baker M. E., Newcombe M. E., Schmidt M. E., Treiman A. H., Cousin A., Dyar M. D., Fisk M. R., Gellert R., King P. L., Leshin L., Maurice S., McLennan S. M., Minitti M. E., Perrett G., Rowland S., Sautter V., Wiens R. C., and M. S. L. Science Team. 2013. The petrochemistry of Jake_M: A Martian mugearite. *Science* 341:6153. doi:10.1126/science.1239463.

Stolper E. M., Baker M. B., Newcombe M. E., Schmidt M. E., Treiman A. H., Cousin A., Dyar M. D., Fisk M. R., Gellert R., King P. L., Leshin L., Maurice S., McLennan S. M., Minitti M. E., Perrett G., Rowland S., Sautter V., Wiens R. C., and the MSL Science Team. 2014. The petrochemistry of Jake_M: A Martian mugearite. *Science* 341, doi:10.1126/science.1239463.

Talbot M. R., Holm K., and Williams M. A. J. 1994. Sedimentation in low-gradient desert margin systems: A comparison of the Late Triassic of northwest Somerset (England) and the late Quaternary of east-central Australia. In *Paleoclimate and Basin Evolution of Playa Systems*, edited by Michael R. Rose. *Geological Society of America Special Papers* 289:97–117. doi:10.1130/SPE289-p97.

Thomson B. J., Bridges N. T., Milliken R., Baldrige A., Hook S. J., Crowley J. K., Marion G. M., de Souza Filho C. R., Brwon A. J., and Weitz C. M. 2011. Constraints on the origin and evolution of the layered mound in Gale Crater, Mars using Mars Reconaissance Orbiter data. *Icarus* 214:413–432. doi: 10.1016/j.icarus.2011.05.002.

Toner J. D., Catling D. C., and Light B. 2015. Modeling salt precipitation from brines on Mars: Evaporation versus freezing origin for soil salts. *Icarus* 250:451–461.

Tosca N. J. and McLennan S. M. 2009. Experimental constraints on the evaporation of partially oxidized acid-sulfate waters at the Martian surface. *Geochimica et Cosmochimica Acta* 73:1205–1222.

Tosca N. J., McLennan S. M., Lindsley D. H., and Schoonen M. H. 2004. Acid-sulfate weathering of synthetic Martian basalt: The acid fog model revisited. *Journal of Geophysical Research* 109:E05003. doi:10.1029/2003 JE002218.

Tosca N. J., Knoll A. H., and McLennan S. 2008. Water activity and the challenge for life on early Mars. *Science* 320:1204–1207.

Treiman A. H. 2005. The nakhlite meteorites: Augite-rich igneous rocks from Mars. *Chemie der Erde* 65:203–270.

Turner S. M. R., Hansford G. M., Bridges J. C., Ambrosi R. M., and Vernon D. 2013. A study of sulphate minerals using a novel X-ray diffraction technique. EPSC abstracts, Vol. 8, EPSC2013-379-2.

Van Berk W. and Fu Y. 2011. Reproducing hydrogeochemical conditions triggering the formation of carbonate and phyllosilicate alteration mineral assemblages on Mars (Nili Fossae region). *Journal of Geophysical Research* 116:16 p. doi:10.1029/2011JE003886.

Van Driessche A. E. S., Benning L. G., Rodriguez-Blanco J. D., Ossorio M., Bots P., and Garcia-Ruiz J. M. 2012. The role and implications of Bassanite as a stable precursor phase to gypsum precipitation. *Science* 336:69–72. doi:10.1126/science.1215648.

Vaniman D. T., Bish D. L., Chipera S. J., Fialips C. I., Carey W., and Feldman W. C. 2004. Magnesium sulphate salts and the history of water on Mars. *Nature* 431:663–665.

Vaniman D. T., Bish D. L., and Chipera S. J. 2009. Bassanite on Mars (abstract #1654). 40th Lunar and Planetary Science Conference. CD-ROM.

Vaniman D. T., Bish D. L., Ming D. W., Bristow T. F., Morris R. V., Blake D. F., Chipera S. J., Morrison S. M., Treiman A. H., Rampe E. B., Rice M., Achilles C. N., Grotzinger J., McLennan S. M., Williams J., Bell J. III, Newsom H., Downs R. T., Maurice S., Sarrazin P., Yen A. S., Morookian J. M., Farmer J. D., Stack K., Milliken R. E., Ehlmann B., Sumner D. Y., Berger G., Crisp J. A., Hurowitz J. A., Anderson R., DesMarais D., Stolper E. M., Edgett K. S., Gupta S., and Spanovich N. 2014. Mineralogy of a mudstone on Mars. *Science* 343: doi:10.1126/science1243480.

Vaniman D. T, Blake D. F., Bristow T. F., Chipera S., Gellert R., Ming D., Morris R., Rampe E. B., and Rapin W. 2015. Diagenetic mineralogy at Gale Crater, Mars. Abstract 266820, Geological Society of America Meeting and Exposition.

Vasavada A. R., Grotzinger J. P., Arvidson R. E., Calef F. J., Crisp J. A., Gupta S., Hurowitz J., Mangold N., Maurice S., Schmidt M. E., Wiens R. C., Williams R. M. E., and Yingst R. A. 2014. Overview of the Mars Science Laboratory mission: Bradbury Landing to Yellowknife Bay and beyond. *Journal of Geophysical Research: Planets* 119:1134–1161. doi:10.1002/2014JE004622.

Villanueva G. L., Mumma M. J., Novak R. E., Käufl H. U., Hartogh P., Encrenaz T., Tokunaga A., Khayat A., and Smith M. D. 2015. Strong water isotopic anomalies in the Martian atmosphere: Probing current and ancient reservoirs. *Science* 348:218–221.

Wang A., Haskin L. A., Squyres S. W., Joliff B. L., Crumpler L., Gellert R., Schröder C., Herkenhoff K., Hurowitz J., Tosca N. J., Farrand W. H., Anderson R., and Knudson A. T. 2006. Sulfate deposition in subsurface regolith in Gusev Crater, Mars. *Journal of Geophysical Research Letters* 111:19 p. doi:10.1029/2005JE002513.

Warrington G., Ivimey-Cook H. C., Edwards R. A., and Whittaker A. 1995. The Late Triassic–Early Jurrassic succession at Selworthy, West Sommerset, England. Annual Conference of the Ussher Society, January 1995. http://ussher.org.uk/journal/90s/1995/documents/Warrington_et_al_1995.pdf

Watson J. S., Gilmour I., Jolley D. W., Kelley S. P., Gilmour M. A., and Gurov E. P. 2010. Molecular parameters of post impact cooling in the Boltysh impact structure. 41st Lunar and Planetary Science Conference. CD-ROM.

Westall F., Foucher F., Bost N., Bertrand M., Loizeau D., Vago J. L., Kminek G., Gaboyer F., Campbell K. A., Bréhéret J.-B., Gautret P., and Cockell C. S. 2015. Biosignatures on Mars: What, where and how? Implications for the search for Martian life. *Astrobiology* 15:998–1029.

Wiens R. C., Maurice S., Gasnault O., Clegg S., Fabre C., Nachon M., Rubin D., Goetz W., Mangold N., derSchrö S., Rapin W., Milliken R., Fairén A. G., Oehler D., Forni O., Sautter V., Blaney D., Le Mouelic S., Anderson R. B., Cousin A., Vasavada A., Grotzinger J., and the MSL Science Team. 2015. Centimeter to decimeter sized

spherical and cylindrical features in Gale Crater sediments (abstract #1249). 46th Lunar and Planetary Science Conference. CD-ROM.

Williams F. A., Kelley S. P., Gilmour I., Jolley D. W., and Gilmour M. 2013a. The Boltysh impact crater, Ukraine: smectites from the crater-fill suevites. In: European Planetary Science Congress 2013, 08–13 September 2013, London.

Williams R. M. E., Grotzinger J. P., Dietrich W. E., Gupta S., Sumner D. Y., Mangold N., Malin M. C., Forni O., Ollila A., Newsom H., Dromart G., Palucis M. C., Yingst R. A., Anderson R., Herkenhoff K., Le Mouelic S., Stack K., Madsen M., Koefoed A., Jensen J. K., Goetz W., Bridges J. C., Schwenzer S. P., Rubin D., Pariser O., Deen R. G., and the MSL Science Team. 2013b. Martian fluvial conglomerates at Gale Crater. *Science* 340:1068–1072.

Zolotov M. Y. and Mironenko M. V. 2007. Timing of acid weathering on Mars: A kinetic-thermodynamic assessment. *Journal of Geophysical Research* 112:20 p. doi:10.1029/2006JE002882.